## MINISTRY OF NATIONAL EDUCATION AND SCIENTIFIC RESEARCH TECHNICAL UNIVERSITY OF CIVIL ENGINEERING BUCHAREST DOCTORAL SCHOOL

### PhD THESIS

- SUMMARY -

# SIMULATION OF ACCELEROGRAMS SPECIFIC TO VRANCEA INTERMEDIATE-DEPTH SEISMIC SOURCE

PhD Student:

Eng. Eliza-Anabella COŢOVANU

PhD Supervisor:

Prof. PhD.eng. Radu VACAREANU

BUCHAREST 2020

### **Table of contents**

1. Introduction	3
1.1. Necessity and object of the thesis	3
1.2. Content of the thesis	
2. Simulation of ground motions generated by Vrancea intermediate-depth seismic source.	
Simulation methods. Pros and cons	6
2.1. Simulation of ground motions produced by the Vrancea intermediate-depth earthquak	e of
October 27, 2004	
2.2. Simulation of ground motions produced by the Vrancea intermediate-depth earthquak	e of
August 30, 1986	
2.3. Conclusion for simulation methods. Pros and cons	17
3. Modeling energy release parameters in stochastic simulation of ground motions generated by	,
Vrancea intermediate-depth seismic source. Mathematical modeling of the shaping window	
3.1. Introduction	
3.2. The energy release of recorded ground motions during Vrancea intermediate-d	lepth
earthquakes	
3.3. The mathematical model of the shaping window implemented in SMSIM and EXS	SIM.
Determining the window parameters	
3.3.1. The mathematical model of the shaping window implemented in SMSIM and EXSI	M 22
3.4. Defining a two intervals shaping window that can describe the specific energy releas	se of
ground motions generated by Vrancea intermediate-depth strong earthquakes	26
3.4.1. Continuity and derivability issues in modeling the energy release shaping window	26
3.4.2. Defining the window function's intervals	27
3.4.3. Defining the new envelope function after the model proposed by Sharagoni și	
(1974) 28	
3.4.4. Redefining parameters for the time normalized form proposed after Boore (2003)	29
3.5. Simulations in SMSIM using the newly defined window function	30
3.6. Conclusions	32
4. Defining the parameters of the seismic action used in the simulation of ground motions	
generated by Vrancea intermediate-depth seismic source	34
4.1. Introduction	34
4.2. The locations of the Vrancea intermediate-depth earthquakes	35
4.3. Path duration	37
4.4. Conclusions	39
5. Simulation of accelerograms specific to Vrancea intermediate-depth major seismic events	42
5.1. Introduction	
5.2. Simulation of the INCERC site accelerograms generated by the Vrancean intermed	iate-
depth earthquake of August 30, 1986	43
5.3. Simulation of the INCERC site accelerograms generated by the Vrancean intermed	iate-
depth earthquake of March 4, 1977	45
5.4. Simulation of the INCERC site accelerograms generated by some Vrancean intermed	iate-
depth scenario earthquakes	
5.5. Conclusions	55
6. Conclusions, personal contributions and future research directions	56
7. Bibliography	59

### 1. Introduction

### 1.1. Necessity and object of the thesis

The most influential natural hazard action to which the structures and the buildings in Romania are designed is the seismic action. The territory of the country has a seismic hazard influenced by the following seismogenic zones: Intermediate-Vrancea, Crustal-Vrancea, Bârlad's Depression, Predobrogean Depression, Făgăraș-Câmpulung, Transylvania, Danubius, Banat, Crișana-Maramureș, Serbia, Gorna, Shumen, Dulel and Shabla, (Pavel, et al., 2016). Romania is considered one of the countries with the highest level of seismic hazard in Europe. Of these seismogenic zones, the one with the most extensive territorial effect is Vrancea intermediate-depth source (this being the subject of the present work), which affects two thirds of the territory of Romania, its effects being felt from Bulgaria to Russia.

For the analysis of the seismic response of structures, the National code for anti-seismic design P100-1/2013 (MDRAP, 2014) proposes three calculation methods: the method of equivalent static seismic forces, the method of modal calculation with response spectra and the dynamic calculation method. For the first two methods, the seismic action can be determined by combining the design acceleration and the normalized elastic response spectra, but for the dynamic calculation the seismic action must be described by the time series ground accelerations (accelerograms), a minimum of 3 accelerograms being required to perform the analysis.

The recorded accelerograms can be used if they are compatible with the characteristics of the source (type and rupture mechanism), the position of the site analysed relative to the hypocenter, and the local site conditions; the peak value of the ground acceleration must correspond to the hazard level given in P100-1/2013 (MDRAP, 2014) and the frequency content of the motion must be in accordance with the elastic response spectrum corresponding to the analysed site. For the use of the recorded accelerograms a scaling factor of the acceleration values can be used to reach the proposed hazard level of the code, but its value must be less than 2.0. Due to the fact that only four seismic events with a minimum magnitude of 6.3 were recorded, there are few recorded accelerograms that fulfil the conditions imposed by the design code; therefore, one may need to use artificial or simulated accelerograms.

Nationally, the most used accelerograms are the artificial ones because they are obtained relatively simply by a method of matching their spectra with the elastic response spectrum for accelerations from the site of interest. The advantage is that their generation does not require an indepth knowledge of the physical phenomena that produce and influence the seismic waves. However, the artificial accelerograms have no real physical significance, the non-stationarity of the seismic motion is not reproduced, their frequency content is unrealistic and they introduce a highly unrealistic energy into the structure.

Under these conditions, an alternative for avoiding inconsistencies produced by artificial accelerograms is the use of simulated accelerograms that can easily meet the normative conditions without introducing an energy surplus in the structure, while preserving their physical significance. The simulated accelerograms are generated based on the real phenomena that produce and influence the seismic waves. However, they are not widely used because they require a deep knowledge of the

factors that influence the seismic motion and their quantification models are more complex than in the case of artificial accelerograms.

Currently, there are four methods for generating simulated accelerograms: the empirical Green's function method, stochastic modeling, numerical modeling and hybrid methods. The use of a certain method is dependent on the level of knowledge of the processes of generation and modification of the seismic waves and on the applicability of the principles of the methods for the seismogenic zones for which the simulations are performed. At present, stochastic modeling is the most accessible simulation method for the intermediate-depth Vrancea seismogenic source. For applying the method one should know the characteristics of the material in the vicinity of the hypocenters (velocity and density), the focal mechanism, the released energy, the radiation pattern, the spectral characteristics of the motion in the vicinity of the source, the durations of the source and the path, the attenuations and scatterings produced by propagation environments traveled by the seismic waves, the behavior of surface geological layers, etc. However, under certain conditions of hazard level, surface geology or topography, the stochastic approach fails to model all the physical phenomena that influence seismic waves. Under these conditions, hybrid methods that combine stochastic and numerical modeling can be used to successfully obtain simulated accelerograms

In the present paper, a hybrid method of generating the simulated accelerograms is modified and applied. Based on thorough research, simulations for the ground motions generated by Vrancea intermediate-depth source are successfully performed for both seismic motions generated by past events and for earthquake scenarios defined in such a way as to correspond to the hazard level from the Design Code P100-1/2013 (MDRAP, 2014). The usefulness of the simulated accelerograms is given both by the possibility of their use in the design of structures in dynamic calculation method, as well as by the possibility of using them together with the recorded accelerograms in hazard analyses (by simulating unregistered historical events, or by simulating possible hypothetical events through which can cover ranges of magnitude not covered by actual events, and for locations where there is no recorded ground motions).

#### 1.2. Content of the thesis

The thesis "Simulation of ground motions generated by Vrancea intermediate-depth seismic source" contains 6 chapters, 3 annexes (Annex 3 is in electronic format), 262 pages and 170 bibliographic references.

*Chapter 1* briefly presents the content of the paper, the objective of the thesis and the necessity of researching the subject.

Chapter 2 presents the ground motion simulation methods, a state of the art in the subject for seismic events that contribute to the seismic hazard in Romania, the results of some simulations based on stochastic and hybrid simulation methods, comparative analyses of simulations with real motions, and pros and cons of the applied methods. This chapter contains analyses of some parameters and models that contribute to the generation of simulated accelerograms. In this stage, it is discovered that the mathematical model for shaping the generated noise (which is subsequently loaded with the characteristics of the events) does not capture the specificity of the seismic motions produced by the Vrancea intermediate-depth earthquakes.

Chapter 3 presents an analysis of the energy release described by 361 records of seismic motions during the earthquakes of March 4, 1977, August 30, 1986, May 30, 1990, May 31, 1990, and October 27, 2004. It was observed that almost half of the analysed accelerograms exhibit a fast release of a large amount of energy, followed by a considerably slower release (about 50% of the energy is released in the first 1.5-3.0 s of the strong motion, while the rest of the energy is released slowly in 20-40 s). Based on the statistical descriptors resulted from the analysis of the accelerograms that presented the aforementioned behaviour, the parameters of the noise shaping window implemented in the stochastic simulation programs used in the thesis were determined. Noting that the mathematical model of the implemented window cannot capture the two types of energy release, a new mathematical model of the shaping window specific to the Vrancea intermediate-depth source motions was defined and implemented in one of the simulation programs. For the new defined shaping window, the expected parameters have been determined so that they can be used for hypothetical earthquake scenarios.

Chapter 4 contains an elaborate research of all the input parameters and the models for defining the phenomena that modify and generate the seismic waves. For the parameters for which in the specialized literature there were several variants of definition comparative analyses were performed and the most suitable model was chosen for the description of the respective phenomenon in the stochastic simulations. For the parameters for which there are no specific studies, or for which the definition intervals were too wide and this would have introduced errors in simulation, specific studies were performed and models for simulations were defined. Also in this chapter, four possible earthquake scenarios spatial intervals were defined and the related simulation parameters were given.

In *Chapter 5*, ground motions simulations for the INCERC site (Bucharest) produced by the seismic events of March 4, 1977, August 30, 1986, four earthquake scenarios defined in accordance with the maximum scenarios of Chapter 4 and four earthquake scenarios defined according to the principles of design from P100-1 / 2013 were performed. For the simulation, a hybrid method composed of a modified stochastic method for simulating accelerograms up to the bedrock level and a numerical method to simulate the behaviour and influence of local site conditions was used. The simulations based on real earthquakes had the purpose of testing the method and analysing some hypotheses regarding the values of the parameters used in the analysis, their results being very good. Based on the verified method, the simulations of seismic motions generated in accordance with the characteristics of some earthquake scenarios were performed and comparisons were made with the hazard level proposed by Design Code P100-1/2013. The accelerograms simulated based on the design requirements are annexed to the PhD thesis in electronic format.

Chapter 6 contains the general conclusions of the paper, personal contributions and future research directions.

### 2. Simulation of ground motions generated by Vrancea intermediatedepth seismic source. Simulation methods. Pros and cons

Currently, there are four main methods for simulating time series seismic motions: by stochastic models, by the empirical Green's function method, by using numerical models based on physical characteristics and by hybrid methods that combine numerical modeling, the empirical Green's function method and stochastic modeling.

### The empirical Green's function method

Since a large magnitude earthquake is characterized by a large rupture surface and a small magnitude earthquake is characterized by a small rupture surface, the empirical Green's function method is based on the hypothesis that a large rupture surface can be modelled with several small rupture surfaces. Thus, the method proposes to model the high magnitude earthquake through several small magnitude earthquakes, considered as point sources along the rupture surface. The ground motion generated by the large event can be described by the sum of some motions generated by small events that takes into account the phase differences due to the propagation of the rupture and the differences in the frequency content between the two types of seismic events. The advantage of using this method is given by the fact that the seismic motions generated by the small events (Green functions) contain the characteristics of the fault geometry, the characteristics of wave propagation and, under certain conditions, the influence of the local site conditions. The basic works in the specialized literature on the method are Hartzell (1978), Kanamori (1979), Irikura (1983; 1986; 1999), Miyake et al. (2003).

### Time series stochastic simulation method

Hanks and McGuire (1981) demonstrate that high-frequency accelerations can be described as Gaussian noise (with a normal probability distribution) over a limited frequency band, with certain spectral characteristics. It can also be assumed that the acceleration phase of the seismic motion is random. Thus, they combined spectral amplitude models of the seismic motion with the hypothesis that, in practice, high-frequency motions are random (Hanks, 1979; McGuire & Hanks, 1980; Hanks & McGuire, 1981). Boore (1983) generalized the previous approach to allow the use of more complex, extended models to simulate time series in which more features of the seismic motion can be considered. The equation of the spectrum of the seismic motion used by Boore (2003) is as follows:

$$Y(M_0 R, f) = E(M_0, f)P(R, f)G(f)I(f)$$
(1)

where  $M_0$  - is the seismic moment, expressed in Nm (Aki, 1966), the transformation between the seismic moment and the moment magnitude is given by the relation  $M_w = \frac{2}{3} \log M_0 - 10.7$ ; E - the function that describes the source mechanism; P - the function that describes the influence of wave propagation media; G - the function describing the influence of local site conditions; I - the function that controls the type of the result.

In the specialized literature one can find, for the modeling of the seismic source, two methods: point source stochastic modeling and finite source stochastic modeling.

### **Numerical modeling. Theoretical simulations (3D)**

The most appropriate method for simulating long-period ground motions is the fourth order finite difference method with spatial grid variables (Pitarka, 1999) and the frequency-dependent attenuation factor (Irikura & Miyake, 2006). The 3D numerical method is used in particular to simulate ground motions in the sedimentary basin areas because it is the only one that can model seismic wave reflections and refractions. This method involves constructing a 3D velocity model for describing all the geological layers crossed by seismic waves and determining the optimal attenuation parameter, the resulting waves being 3D. Wave propagation is analysed in a 3D linear-elastic isotropic environment and is defined by the equations for moment conservation and stress-strain relationships.

### **Hybrid methods**

The simulation of the seismic motion produced by a large event near the source has a good accuracy if there is a detailed knowledge about the source mechanism and the geological configuration of the stratifications crossed by the seismic waves from the source to the surface. Thus, hybrid simulation methods have been developed, and they combine the stochastic and the deterministic methods. Long-period motions given by a large earthquake can be simulated by deterministic methods, and short-period motions can also be simulated using either stochastic methods (e.g. Boore, 2003) suitable for small earthquakes, or using empirical Green's function method (e.g. Irikura 1986) suitable for large earthquakes. The simulated seismic motion results from the summation of long-period and short-period motions after their filtering.

### Application of simulation methods for seismogenic sources that contribute to the seismic hazard in Romania

In Romania, accelerogram simulations were performed only for Vrancea intermediate-depth source. The simulations were generated using the empirical Green's function method, the time series stochastic simulation method and hybrid methods which involve the use of the stochastic method up to the bedrock level and the deterministic analytical method (numerical) to include the influence of local site conditions. Benetatos and Kiratzi (2004) use the finite fault stochastic simulation method to generate the seismic motions produced by the earthquake of May 30, 1990 (Mw = 6.9). Oth et al. (2009) use the empirical Green's function method to simulate the seismic motions produced by the earthquakes of March 4, 1977 (Mw = 7.4), August 30, 1986 (Mw = 7.1), October 27, 2004 (Mw = 6.0) and May 14, 2005 (Mw = 5.2). Pavel (2015) uses the point source stochastic method to simulate the seismic motions generated by the earthquakes of August 1986 and May 1990. Pavel and Vacareanu (2015) simulate the motions produced by the earthquakes of November 1940 (Mw = 7.7) and March 1977 by a hybrid method that combines the point source stochastic method and a numerical method for quantifying the effects of local site conditions. Poiată and Miyake (2017) perform simulations of the motions produced by the earthquakes of 1977 and 2004 using the empirical Green's function method. Pavel (2017) and Pavel and Vacareanu (2017) simulate, using the finite fault stochastic method, ground motions produced by hypothetical events with moment magnitudes with values in the range 5.5-7.5. Pavel et al. (2018) simulate the motions produced by hypothetical events with magnitudes with values between 5.5-7.5 using the finite fault stochastic method and the numerical modeling for taking into account the influence of local site conditions.

The main problems raised in these works are related to quantifying the effect of local site conditions, using various methods to determine their influence (by amplification functions, by the H/V spectral ratio, by the impedance calculation or by the use of linear—equivalent or nonlinear analysis programs). An inconsistency observed in the studies is represented by the definition of the stress drop parameter which in the work of Oth et al. (2009) is considered with a value of the 1000 bars order, and in the specialized literature it is found having values about 10 times smaller.

In this chapter, in order to determine the best method for simulating the accelerograms specific to Vrancea intermediate-depth earthquakes, simulation sets were generated for the INCERC site (Bucharest) using the characteristics of the earthquakes of October 27, 2004 (Mw = 6.0, h = 105 km) and from August 30, 1986 (Mw = 7.1, h = 131 km). To define the local site conditions, the H/V method, the impedance contrast method and the nonlinear soil analysis were used. Also for the 2004 earthquake an analysis was performed on the stress drop parameter. The 2004 earthquake was chosen as a target event because the nonlinear behaviour of the surface geological stratification specific to the INCERC site (Bucharest) during this earthquake can be neglected. Based on these simulations, comparative analyses were performed between the point source, finite fault stochastic methods and the hybrid methods formed from the two stochastic methods and the numerical method of quantifying the influence of local site conditions.

Simulations were performed with the following programs: SMSIM (Boore, 2005), EXSIM (Motazedian & Atkinson, 2005), SITEAMP (Boore, 2005; Boore & Joyner, 1997) and DEEPSOIL (Hashash, et al., 2016). The first two sets of programs use the stochastic method to simulate time series ground motions, in the SMSIM the source is defined as a point source, and in the EXSIM as a finite source. The last two calculation programs model the changes in seismic motions that occur due to local site conditions. The parameters resulting from the use of the SITEAMP set of programs (the result being an amplification profile calculated by impedance, taking into account the linear behaviour of the soil) are input data in SMSIM and EXSIM, while the accelerograms at the bedrock made with SMSIM and EXSIM are input data for DEEPSOIL - by which the influence of the nonlinear behaviour of the superficial geological stratification is quantified.

In the two sets of programs, SMSIM and EXSIM, the local site conditions are modelled using two functions, an amplification function and a frequency-dependent attenuation function. For purely stochastic simulations, an amplification function determined through the H/V ratio (the ratio of the Fourier spectra of the motion in the horizontal and vertical direction) and another one determined through the impedance contrast (using the NRATTLE subprogram from SITEAMP) were used. However, for medium and large earthquakes, some types of soil layers may modify their properties (by increasing the interstitial pressure, increasing or losing shear strength, increasing density, liquefaction, etc.), and in these conditions the nonlinear behaviour must be taken into account. For this matter, for the nonlinear analysis in the time domain, the DEEPSOIL program was used.

For both stochastic simulation programs, the seismic motion spectrum and the noise shaping window are defined using the same type of parameters and the same type of modeling of the phenomena that influence the seismic wave. The source spectrum definition is the only difference between the programs. The spectrum of the seismic motion  $Y(M_0,R,f)$  (equation 1) contains three components that carry the characteristics of the source  $E(M_0,f)$ , the influence of the propagation path crossed by waves P(R,f) and influence of local site conditions G(f).

### 2.1. Simulation of ground motions produced by the Vrancea intermediate-depth earthquake of October 27, 2004

The seismic event of October 27, 2004 was a medium earthquake having a magnitude of 6.0 with the focal depth of 105.4 km and the epicenter at 45.84° N latitude and 26.63° E longitude (Radulian, et al., 2019). The dimensions of the rupture plane (seismic fault), according to Oth et al. (2007), were 1.2 x 1.8 km, and the stress drop parameter was 75 bars (Ganas, et al., 2010). The focal mechanism, according to Ganas et al. (2010), is characterized by a 219° strike, an 81° dip, and a 107° rake.

For the average velocity of shear waves  $\beta_s$  and density  $\rho$  near the source, in the literature, there are several values, thus Martin et al. (2006) propose  $\beta_s = 4.5$  km/s and  $\rho = 3.2$  g/cm<sup>3</sup>, and Sokolov et al. (2008) propose  $\beta_s = 3.8$  km/s and  $\rho = 2.8$  g/cm<sup>3</sup>. For calibration reasons, in the simulation the average velocity of the shear waves  $\beta_s = 4.5$  km/s and the density  $\rho = 2.8$  g/cm<sup>3</sup> were considered. For the calculation of the C constant, the following values were considered: the average radiation pattern  $\langle R_{\theta\Phi} \rangle$  was considered 0.6, according to Oth et al. (2008), the horizontal component V of the total energy of the shear waves given by the two-way decomposition being  $1/\sqrt{2}$ , the effect of the free surface is 2, and the reference distance was considered 1 km.

For the path influence, Pavel and Vacareanu (2015) observed that, for long and medium frequencies, the form  $1/R^{0.5}$  has a good match for the scattering  $(R = \sqrt{D^2 + h^2})$ .

For the source to site distance, two sets of simulations were performed: one for R=186~km (considering D=154~km - the epicentral distance to INCERC Bucharest- and h=105.4~km) and another one for  $R_{eff}=191~km$  - effective distance which takes into account the fault geometry (resulting from reff.exe, an executable within the SMSIM set of programs). Regarding the attenuation, in Pavel and Vacareanu (2015) it was determined as having the form  $Q(f)=100~x~f^{1.20}$ .

To model the diminution effects, Radulian et al. (2000) observed a significant dependence of the parameter k on the magnitude of the earthquakes and on the local site conditions. For example, for the Bucharest area the average value  $k_0$  is relatively high 0.071, in the Moldavian area the average value  $k_0$  is 0.057, and in the epicentral area  $k_0$  has an average value of 0.101. For simulation, the kappa parameter values were considered from Pavel and Vacareanu (2015) paper, which used the estimation method proposed by Anderson and Hougs (1984), to determine the value of the kappa parameter as  $k = k_{event} + k_0$ , where  $k_{event} = 0.022M_w - 0.127$ . Another study, conducted by Sokolov et al. (2008), provides a relation for the kappa parameter as  $k = 0.01M_w$ . The source duration was considered according to Boore (2003), and the path-dependent duration was considered 0.0868 according to Pavel (2015). For the shear wave profile for the INCERC site (Bucharest), the stratification proposed by Constantinescu and Enescu (1985) was used.

For the point-type source spectrum (SMSIM) there are three types of definition: through a single-corner frequency spectrum, through an additive spectrum with two corner frequencies and through a multiplicative spectrum with two corner frequencies. The common characteristics of all the spectra are given by the fact that for low frequencies the amplitude increases proportionally with the seismic moment, and that for high frequencies the spectrum becomes flat, with an amplitude equal to that of the model with a single corner frequency.

Simulations were performed for 3 types of source spectra: with a single corner frequency (Source 1, S1), and with two corner frequencies with multiplicative spectrum (Source 11, S11) and additive spectrum (Source 12, S12). To define the sources, the following models were used:  $\omega^2$  model for Source 1 (Brune, 1970; 1971), H96 for Source 11 (Haddon, 1996) and AB95 for Source 12 (Atkinson & Boore, 1995) (table 2). The corner frequency was defined according to Gusev et al. (2002) depending on the moment magnitude according to the relation  $M_w$ =-2 $log(f_c)$ +4.84. For this type of simulation, several sets of simulations were performed. Various hypotheses were tested for the stress drop parameter, the type of the source to site distance, the shaping window through which the release of energy is modelled and for the quantification of local site condition effects. The results of the last set of simulations are presented in figure 1 and table 1 (intermediate steps leading to the selection of some hypotheses over others, eg. in the end only the effective distance was considered).

Using the finite fault stochastic method implemented in EXSIM, two types of simulations were performed for each local site amplification profile. In one type of simulation static subfaults were used, and in the other type of simulation 50% of the subfaults were defined as pulsing (this definition eliminates the dependence of the simulations on the number of subfaults). The results are shown in Figures 2 and 3 and Table 2.

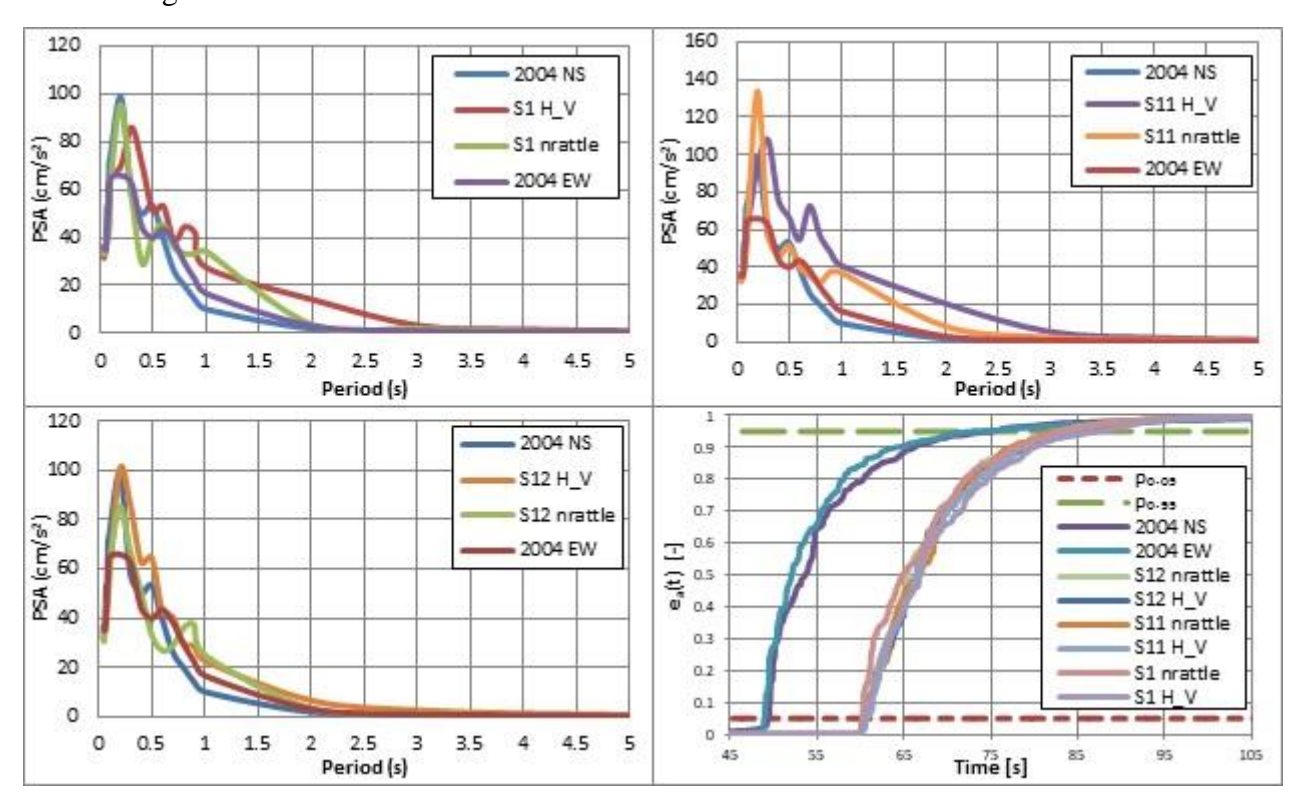


Figure 1. Comparison between the normalized cumulative energies and the response spectra of the simulations and those of ground motions recorded at the INCERC station (Bucharest) during the October 27, 2004 earthquake - the final simulations generated for the S1, S11, S12 sources (Cotovanu, 2018)

Table 1. Characteristics of the ground motions simulated with SMSIM for the earthquake of October 27, 2004, INCERC station(Cotovanu, 2018)

		PGA –			Source		Root mean
	Average	analysed	Source	Path	and path		square
Simulation	PGA	accelerogram	duration	duration	duration	Significant	acceleration
type	$(cm/s^2)$	$(cm/s^2)$	(s)	(s)	(s)	duration (s)	$(cm/s^2)$
S1 H/V	39.7	29.8	1.91	16.92	18.83	22.88	7.9
S1 nrattle	33.1	30.9	1.91	16.92	18.83	22.40	7.1
S11 H/V	42.7	33.6	1.51	16.92	18.43	23.97	9.4
S11 nrattle	34.8	29.6	1.51	16.92	18.43	21.95	8.0
S12 H/V	36.4	31.1	1.94	16.92	18.86	25.04	7.4
S12 nrattle	31.2	29.4	1.94	16.92	18.86	22.11	6.8

Table 2. Characteristics of the ground motions simulated with EXSIM for the earthquake of October 27, 2004, INCERC station(Cotovanu, 2018)

Simulation type	PGA (cm/s <sup>2</sup> )	Significant duration (s)	Root mean square acceleration (cm/s <sup>2</sup> )
2004 NS	29.8	25.65	5.0
2004 EW	30.9	24.80	4.4
EXSIM static nrattle	33.1	11.67	8.1
EXSIM static H/V	35.9	11.11	10.2
EXSIM pulse 50% nrattle	27.8	11.35	7.0
EXSIM pulse 50% H/V	25.5	12.23	7.9

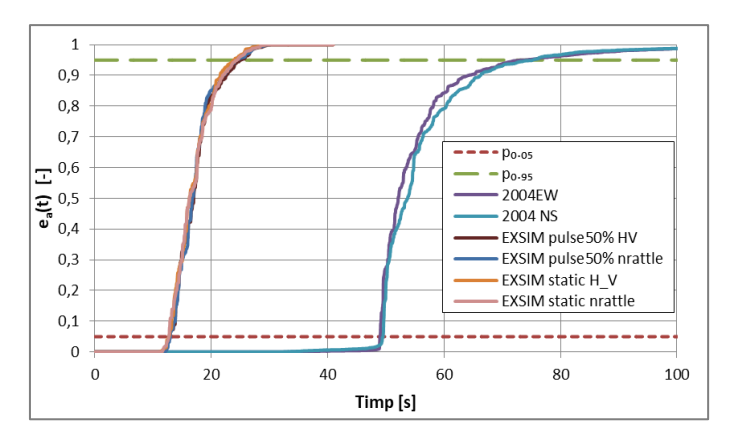


Figure 2. Comparison between the normalized cumulative energies of EXSIM simulations and of ground motions recorded at the INCERC station (Bucharest) during the October 27, 2004 earthquake (Cotovanu, 2018)

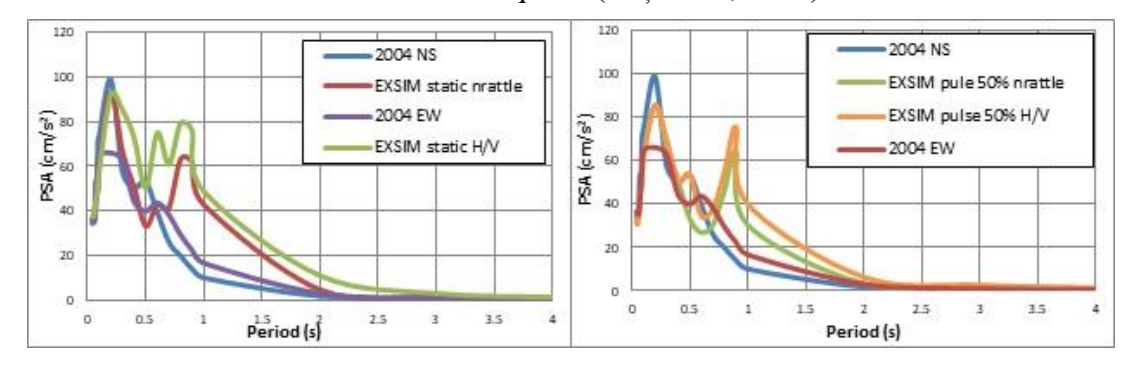


Figure 3. Comparison between the response spectra of EXSIM simulations and of ground motions recorded at INCERC station (Bucharest) during the October 27, 2004 earthquake (Cotovanu, 2018)

### **Findings**

The SMSIM simulations give good estimations of the spectral shape and the peak accelerations, but regarding the intensity, the simulated motions are practically 1.5 times higher. The EXSIM simulations amplify considerably the motion in the 0.5-1.0 s period range, but estimate well the amplitudes corresponding to the small periods, the intensity of the motion being also 1.5-2.0 times higher.

For simulating ground motions produced by medium Vrancea intermediate - depth earthquakes using point source and finite source stochastic methods (implemented in SMSIM and EXSIM programs) estimates well the spectral components corresponding to the periods less than 0.5 s. When generating simulations with SMSIM with an additive source spectrum with two corner frequencies, the simulated accelerograms gave good estimations of the spectral components corresponding the entire 0-4 s range of periods.

The energy release behaviour registered at real motions with a first sudden release segment and a slow and progressive release segment was not captured by any type of simulation.

### 2.2. Simulation of ground motions produced by the Vrancea intermediate-depth earthquake of August 30, 1986

The August 30, 1986 earthquake was a large seismic event with a magnitude of 7.1, the focal being at a depth of 131 km (Radulian, et al., 2019). The simulation of the ground motions generated by this earthquake was mainly performed to investigate the variants by which the influences of the local site conditions can be quantified in the situations in which the superficial geological layers have a nonlinear behaviour.

The following research papers contain ground motion simulations specific to Vrancea intermediate-depth earthquakes for target events that are expected to induce nonlinearity in the superficial soil layers using either purely stochastic methods or hybrid methods that take into quantifying the influence of local site conditions through numerical methods: Benetatos and Kiratzi (2004) have performed simulations using the FINSIM program (Beresnev & Atkinson, 1998) - an older version of the EXSIM program, Pavel (2015) used SMSIM, Pavel and Vacareanu (2015) generated accelerograms using the SMSIM and STRATA programs (Kotke & Rathje, 2009) - a program of soil linear equivalent analysis response, Pavel (2017), Pavel and Vacareanu (2017) used only the EXSIM program and Pavel et al. (2018) used EXSIM and DEEPSOIL - a nonlinear dynamic analysis program (Hashash, et al., 2016).

To compare the capacity of the simulation methods to quantifying the effects of local site conditions, simulations were performed for the INCERC (Bucharest) site using stochastic methods with point source (SMSIM) and finite fault source (EXSIM) in which the site amplifications were defined through the H/V ratio method, the impedance contrast method, and using two hybrid methods in which to the above mentioned stochastic methods were combined with the numerical method implemented in the nonlinear analysis option from DEEPSOIL.

The dimension of the seismic fault according to Oth et al. (2007) was 12.8 x 12.6 km, and the stress drop parameter was 50 bars (Ganas, et al., 2010; Oncescu & Bonjer, 1997). The focal mechanism, according to Ganas et al. (2010) and Oncescu and Bonjer (1997), is characterized by a

strike of  $227^{\circ}$ , a dip of  $65^{\circ}$  and a of  $104^{\circ}$ . In the simulations, the average velocity of the shear waves near the source was considered  $\beta s = 4.5$  km/s and the density near the rupture surface was considered  $\rho = 2.8$  g/cm<sup>3</sup> (Martin, et al., 2006; Sokolov, et al., 2008).

The geometrical scattering was defined as  $1/R^{0.5}$  according to Pavel and Vacareanu (2015). The hypocentral distance was determined taking into account the geometry of the fault, having the value Reff = 182.2 km. The attenuation was considered as Q(f) = 100 x f<sup>1.2</sup> according to Pavel and Vacareanu (2015). The values of the kappa parameter were considered from Pavel and Vacareanu's work (2015) as  $k = k_{event} + k_0$ , unde  $k_{event} = 0.022M_w - 0.127$ . The source duration was defined according to Boore (2003) and the path dependent duration was considered according to Pavel (2015).

For the linear behaviour of soil, two amplification types were considered: the local site amplifications determined using NRATTLE (subprogram from the SITEAMP, SMSIM collection) and the local site amplifications taken from the paper of Pavel (2015) and determined with the H/V ratio method. The nonlinear behaviour of the soil was simulated with DEEPSOIL. The profile of shear waves for the INCERC site (Bucharest) was considered according to Constantinescu and Enescu (1985).

For the point source stochastic method, 3 types of simulations were performed for different source spectrum: with a single corner frequency (S1) and with two corner frequencies with multiplicative spectrum (S11) and additive spectrum (S12). For each definition of the source spectrum, 400 accelerograms were generated using SMSIM with the two types of amplification profiles for the linear behaviour of the soil. The simulation with the closest peak acceleration to the average of the simulation set was analysed. The simulations are illustrated in Figure 4 and Table 3.

Using the finite fault stochastic method implemented in EXSIM, two types of simulations were performed for each linear amplification profile of local site conditions. In one type of simulation static subfaults were used, and in the other type of simulation 50% of the subfaults were defined as pulsating. EXSIM returns a single accelerogram. The results are illustrated in Figures 5, 6 and Table 4.

For the hybrid method, simulations of the seismic motion at the bedrock were performed using SMSIM and EXSIM, and with DEEPSOIL the nonlinear soil behaviour was taken into account for the shear wave profile of the INCERC site proposed by Constantinescu and Enescu (1985). The variation of the stiffness and the damping of the soil layers were adopted for the clay soils according to Vucetic and Dobry (1991), and for the sandy soils according to Seed and Idriss (1970).

For the SMSIM and DEEPSOIL hybrid method, the first set of simulations was performed with the accelerograms with the closest PGA values to the averages of the 400 simulations for each source type, the second with the saved accelerograms that had the maximum PGA, and the third with the saved accelerograms with minimum PGA values. The results are illustrated in Figure 7 and Table 3. Given that the result of the EXSIM program is given by a single output for the hybrid simulations performed with this program and DEEPSOIL, the simulation set contains an accelerogram for the static source and an accelerogram for the pulsing source. The results can be seen in Figure 8 and Table 4.

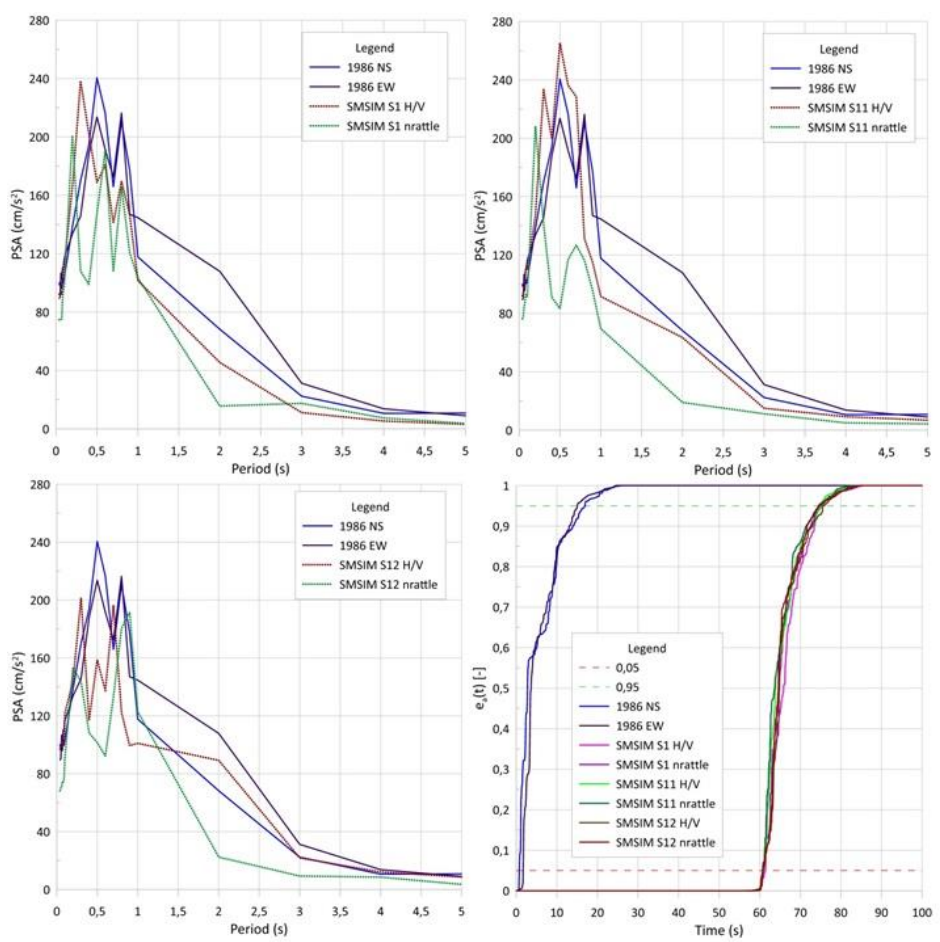


Figure 4. Comparison between the cumulative normalized energies and response spectra of SMSIM simulations and those of the ground motion recordings of August 30, 1986 seismic event at the INCERC (Bucharest) station (Cotovanu & Vacareanu, 2019)

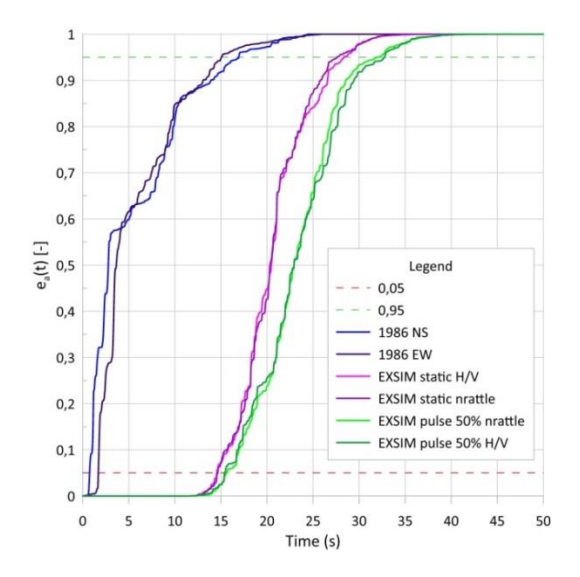


Figure 5. Comparison between the cumulative normalized energies of EXSIM simulations and those of the ground motion recordings of August 30, 1986 seismic event at the INCERC (Bucharest) station (Coţovanu & Vacareanu, 2019)

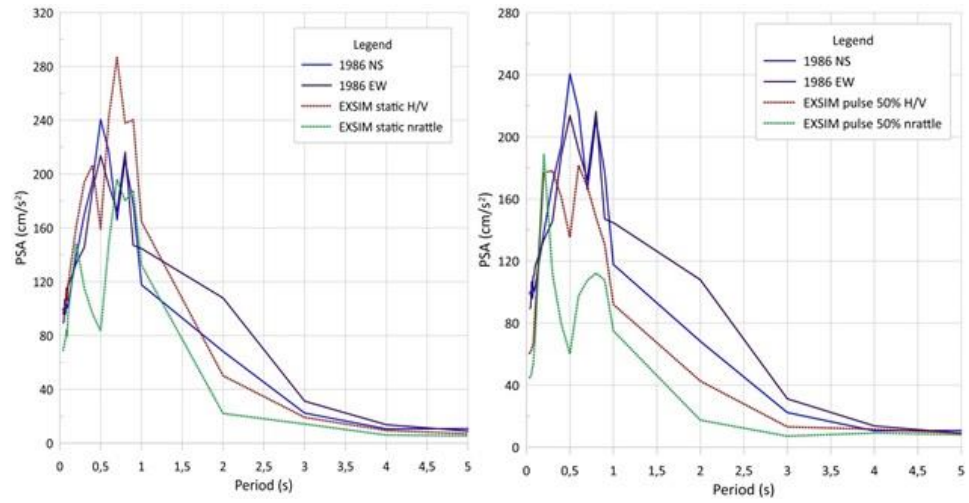


Figure 6. Comparison between the and response spectra of EXSIM simulations and those of the ground motion recordings of August 30, 1986 seismic event at the INCERC (Bucharest) station (Coţovanu & Vacareanu, 2019)

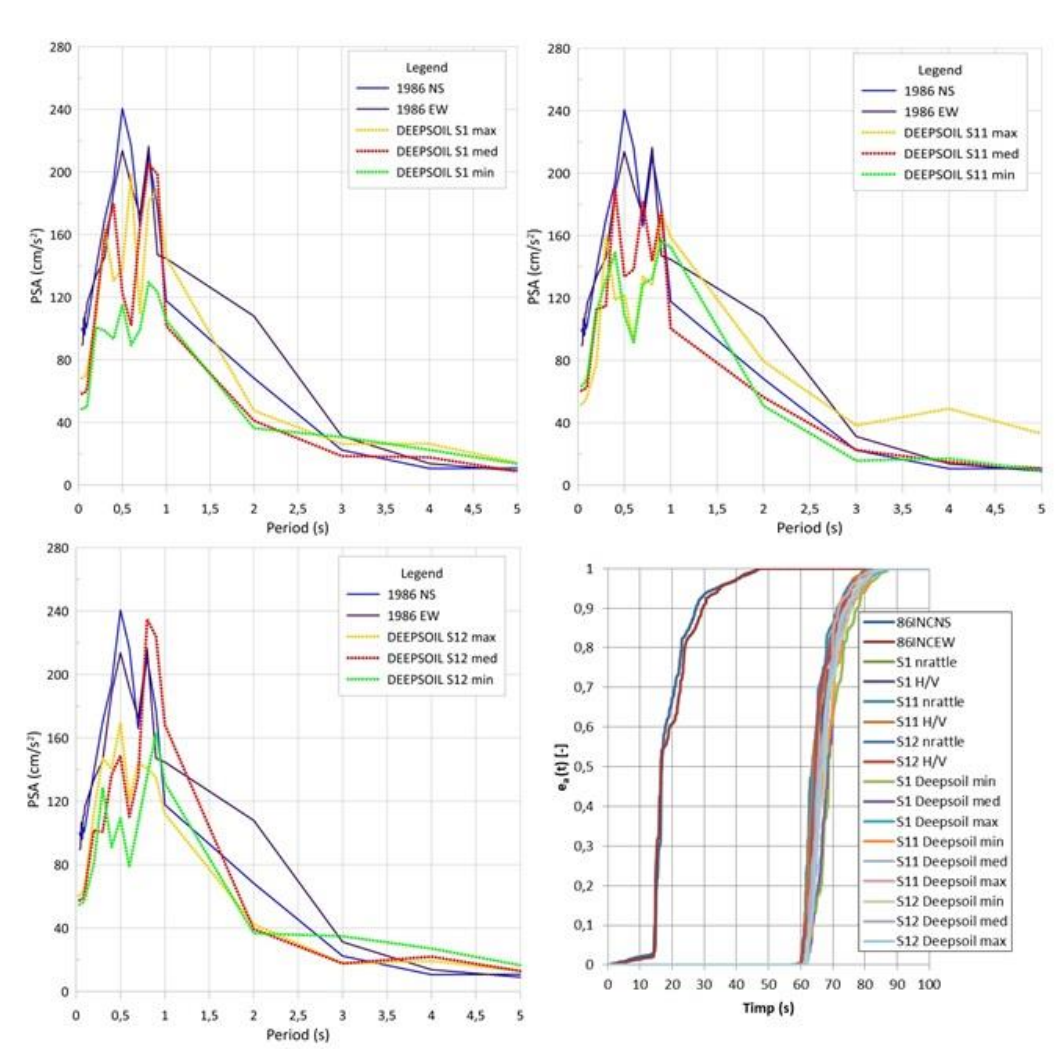


Figure 7. Comparison between the cumulative normalized energies and response spectra of SMSIM and DEEPSOIL simulations and those of the ground motion recordings of August 30, 1986 seismic event at the INCERC (Bucharest) station (Cotovanu & Vacareanu, 2019)

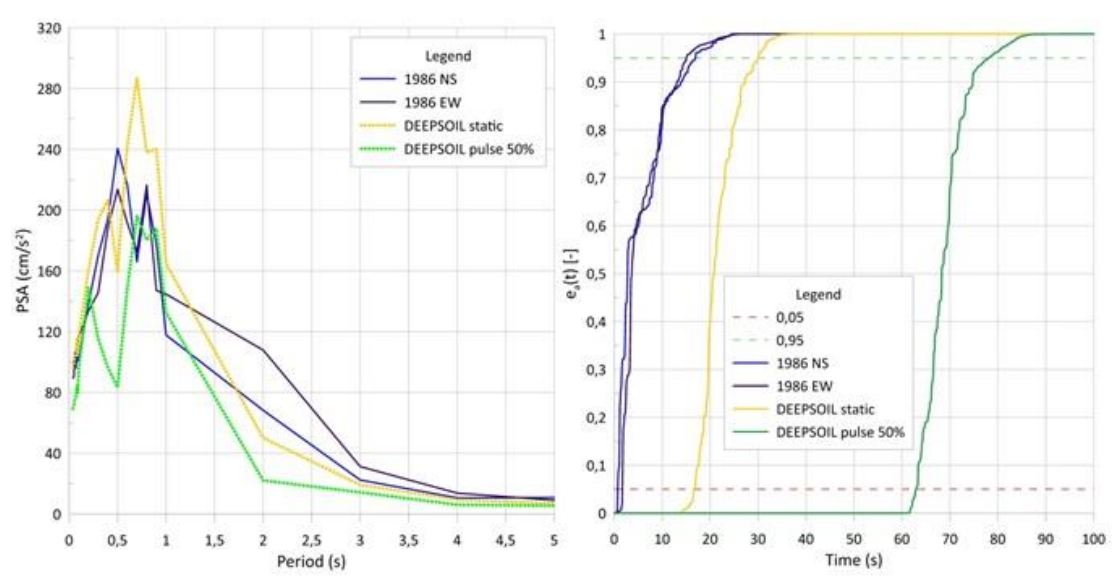


Figure 8. Comparison between the cumulative normalized energies and response spectra of EXSIM and DEEPSOIL simulations and those of the ground motion recordings of August 30, 1986 seismic event at the INCERC (Bucharest) station (Cotovanu & Vacareanu, 2019)

Table 3. Characteristics of the ground motions simulated with SMSIM, and SMSIM and DEEPSOIL for the earthquake of August 30, 1986, INCERC station (Coţovanu & Vacareanu, 2019)

		1		icarcana,	, = /	T .	ī	1	1
		Signific							
	70.1	ant		D 110	D 1711	D 14 11			
G: 1 .:	PGA	duration		DsNS-	DsEW-		ArmsSIM/		ArmsMediu
Simulation type	(cm/s <sup>2</sup> )	(s)	$(cm/s^2)$	DsSIM	DsSIM	-DsSIM	ArmsNS	ArmsEW	/ArmsSIM
1986 NS	96.9	18.9	20.8	0	-1.58	-0.79	1.00	0.92	0.96
1986 EW	109.1	20.48	19.0	1.58	0	0.79	1.09	1.00	1.05
S1 H/V	88.7	13.86	22.1	-5.04	-6.62	-5.83	0.94	0.86	0.90
S1 nrrattle	59.5	14.38	16.7	-4.52	-6.10	-5.31	1.24	1.14	1.19
S11 H/V	90.1	14.21	23.1	-4.69	-6.27	-5.48	0.90	0.82	0.86
S11 nrattle	65.3	14.30	15.3	-4.6	-6.18	-5.39	1.36	1.25	1.30
S12 H/V	89.9	14.94	20.4	-3.96	-5.54	-4.75	1.02	0.94	0.98
S12 nrattle	66.4	13.64	15.5	-5.26	-6.84	-6.05	1.34	1.22	1.28
DEEPSOIL S1 max	67.9	16.69	17.6	-2.21	-3.79	-3.00	1.18	1.08	1.13
DEEPSOIL S1 min	48.5	17.47	13.3	-1.43	-3.01	-2.22	1.56	1.43	1.50
DEEPSOIL S1 med	58.0	15.73	17.2	-3.17	-4.75	-3.96	1.21	1.11	1.16
DEEPSOIL S11 max	51.1	13.34	18.3	-5.56	-7.14	-6.35	1.13	1.04	1.09
DEEPSOIL S11 min	63.0	16.81	16.5	-2.09	-3.67	-2.88	1.26	1.15	1.20
DEEPSOIL S11 med	60.1	15.21	16.2	-3.69	-5.27	-4.48	1.29	1.18	1.23
DEEPSOIL S12 max	60.2	15.80	16.9	-3.1	-4.68	-3.89	1.23	1.13	1.18
DEEPSOIL S12 min	54.4	15.36	15.5	-3.54	-5.12	-4.33	1.34	1.23	1.29
DEEPSOIL S12 med	57.1	15.69	18.1	-3.21	-4.79	-4.00	1.15	1.05	1.10

Table 4. Characteristics of the ground motions simulated with EXSIM, and EXSIM and DEEPSOIL for the earthquake of August 30, 1986, INCERC station (Coţovanu & Vacareanu, 2019)

Simulation type	PGA (cm/s <sup>2</sup> )	Significant duration (s)		DsNS- DsSIM	DsEW- DsSIM	DsMediu- DsSIM	ArmsSIM/ ArmsNS	ArmsSIM/ ArmsEW	ArmsMediu /ArmsSIM
1986 NS	96.9	18.9	20.8	0.00	-1.58	-0.79	1.00	0.92	0.96
1986 EW	109.1	20.48	19.0	1.58	0.00	0.79	1.09	1.00	1.05
EXSIM static nrattle	66.9	12.93	18.0	-5.97	-7.55	-6.76	1.15	1.06	1.11
EXSIM static H/V	94.3	13.79	25.8	-5.11	-6.69	-5.90	0.81	0.74	0.77
EXSIM pulse 50% nrattle	43.0	16.42	13.8	-2.48	-4.06	-3.27	1.51	1.38	1.44
EXSIM pulse 50% H/V	59.9	17.39	19.7	-1.51	-3.09	-2.30	1.06	0.97	1.01
DEEPSOIL pulse 50%	71.6	15.11	22.1	-3.79	-5.37	-4.58	0.94	0.86	0.90
DEEPSOIL static	58.3	13.45	17.6	-5.45	-7.03	-6.24	1.18	1.08	1.13

### **Findings**

Performing simulations that take into account the nonlinear behaviour of the soil leads to a better approximation of the motion for periods less than 1.1 s, but for almost all types of simulations the amplitudes corresponding to periods greater than 1.1 s are underestimated.

The nonlinear behaviour of the soil layers leads to a decrease of the peak values, which means that at the bedrock level the ground motions are greater than those resulting from the simulations performed with SMSIM and EXSIM.

The simulations generated using only SMSIM and EXSIM depend greatly on the chosen amplification profile for describing the superficial soil layers behaviour, which can produce errors (due to the fact that the amplification can be introduced through a limited number of points). This limitation may lead to a selective choice of amplification profile in accordance with a sought behaviour that does not necessarily have a physical justification.

The two-step energy release behaviour is not surprised by any type of simulation. Modeling the energy release closer to the observed behaviour (capturing the pulse – type accelerations) can lead to an increase of peak values at the bedrock, thus increasing the peak values from the surface ground motion after the nonlinear behaviour modeling.

### 2.3. Conclusion for simulation methods. Pros and cons

Simulations were performed for the INCERC (Bucharest) site ground motions generated by two Vrancea intermediate-depth earthquakes, October 27, 2004 (medium event) and August 30, 1986 (large event). The simulations were generated using SMSIM (Boore, 2005), EXSIM (Motazedian & Atkinson, 2005), SITEAMP (Boore & Joyner, 1997; Boore, 2005) and DEEPSOIL (Hashash, et al., 2016). The first two sets of programs contain the stochastic methods, in the SMSIM the source is defined point, and in the EXSIM as a finite fault. The local site conditions were described through amplification profiles determined by the H/V ratio method and by the impedance contrast method (with the SITEAMP program – NRATTLE subprogram) and, for

simulating the nonlinear changes produced by the large event the DEEPSOIL program was used. Based on these simulations, comparative analyses were performed between the stochastic methods with point type source, finite fault type source and the hybrid methods formed from the two stochastic methods and the numerical method of quantifying the influence of local site conditions.

The following were noted:

- a. The stress drop parameter changes the peak values of the motion, the frequency content and the duration of the source.
- b. The use of effective distance  $R_{\text{eff}}$  that takes into account the focal mechanism leads to a better approximation of the seismic motion.
- c. Significant durations and root mean square accelerations are very sensitive to the used window.
- d. The root mean square acceleration is also significantly influenced by the amplification profile used
- e. Geometric scattering greatly influences the peak values of the motions.
- f. For a form of the motion in which high energy is initially released in a short time, and the rest of the energy is released gradually and slower, a two-interval window with two slopes would be required.
- g. For the 2004 earthquake the simulations performed with the NRATTLE amplification profile estimate quite well the motion for all three types of sources. The simulations performed with the H/V profile tend to modify the amplification peaks for longer periods.
- h. For the 2004 earthquake, source 12 is least influenced by the amplification profile of local site conditions.
- i. For large earthquakes, the purely stochastic simulation does not capture the nonlinear behaviour of the soil. Modeling the nonlinear behaviour of the soil leads to better spectral results, but regarding the peak accelerations it underestimates the motion due to the energy dissipation caused by the intrinsic transformations of the soil. For the large seismic event, the motion from the bedrock is most likely larger in peak amplitudes.
- j. In order to obtain simulations that better describe the reality, it is necessary to conduct a more thorough research on all the input parameters considered in simulations.

## 3. Modeling energy release parameters in stochastic simulation of ground motions generated by Vrancea intermediate-depth seismic source. Mathematical modeling of the shaping window

### 3.1. Introduction

Ground motion time-domain stochastic simulations are performed by generating a white or a Gaussian noise, shaping it with a window, loading its normalized spectrum with the spectrum of the motion at a specific site and transforming it back in time-domain (Boore, 2003). The specificity and characteristics of the target ground motions are implemented through the shaping window and the spectrum of the ground motion. The spectrum is divided into four components that contain the characteristics of the source, the influence of the path travelled by the seismic waves, the changes produced by the local site conditions and a filter that controls the type of the result (accelerogram, velocigram or seismogram).

While performing stochastic simulations for ground motions generated by two Vrancea intermediate-depth earthquakes, October 27, 2004 (medium event) and August 30, 1986 (large event) using SMSIM (Boore, 2005) and EXSIM (Motazedian & Atkinson, 2005), it was observed, among others things, that the shaping windows that control the energy distribution in the time domain implemented in the programs cannot capture the specificity of the target motions (where 35-55% of the energy is suddenly released in less than 5 seconds after the limit of 5% of the cumulative energy is reached, while the rest of it, until 95%, is gradually released in 20-40 seconds). The programs have two types of implemented shaping windows: a box and an exponential type. In the simulations only the exponential window was used because it gives the accelerograms a more realistic shape.

This chapter contains two main stages: a first stage in which a set of 371 horizontal components of the recorded ground motions at different stations is analysed to investigate if the previously observed energy release can be found in other locations for other seismic events, and a second stage in which a suitable shaping window for modelling the observed energy release is sought. The analysed horizontal components were registered during the five intermediate-depth Vrancian "modern" earthquakes with a magnitude of at least 6.0 (March 4, 1977, 30 August 1986, May 30 and May 31, 1990, October 27, 2004).

### 3.2. The energy release of recorded ground motions during Vrancea intermediate-depth earthquakes

To investigate if this energy release was specific to the INCERC (Bucharest) station only, a database containing 371 horizontal components of ground motions recorded at different seismic stations during the five earthquakes with moment magnitudes greater than 6.0 produced by the Vrancea intermediate-depth source was analysed. The metadata of these seismic events, as well as the number of records of each event, are given in Table 5. The locations of the stations and the epicentres of the earthquakes can be seen in Figure 9. Since the first objective was to search if the observed energy release pattern can be found in other locations and for the other medium to large Vrancea earthquakes, the database contains accelerograms regardless of the soil conditions or source to site distances.

After processing the cumulative normalized energies for the 371 horizontal components of recorded ground motions at different seismic stations (analysed fraction being 0.05-0.95), five types of energy release patterns (behaviours) resulted, classified as follows: category A or function category (typical pattern for almost half of the records) and category B or exceptions category with type I, II, III and IV exceptions (Figure 10). Category A (most frequent) contains the records where the evolution in time of the cumulative energies has a first abrupt segment where, on average, approximately 50% of the energy is released in the first 1.5-3s of strong motion, and then it has a second segment of 20-40 s where the energy is slowly released until it reaches the threshold of 95% of cumulative energy. Category B, type I exception contains the recordings where the abrupt release of energy is greater than about 70-80% of the total released energy (the percentage depends on the behaviour of cumulative energies intra-earthquake), type II exceptions have a slower than normal release of energy on the second segment (normal refers to the similar behaviour intra-event), type III exceptions have more than two segments of abrupt and slow energy release and type IV exceptions have a slow release of energy from the beginning to the end of the significant duration. Finally, 169 recordings remained in category A from which the window function's parameters where determined. The category B, type I exceptions contains 45 accelerograms, type II contains 25, type III exceptions contains 120 records and type IV contains 12 records.

Table 5. Characteristics of the analysed earthquakes according to ROMPLUS catalogue (Radulian, et al., 2019)

(=, 30 Wii, = 012)									
Crt.	Date	Epicenter	Epicenter	Focal	Moment magnitude	No. of total	Abbreviations for		
no.	Latitude (°N)		Longitude (°E)	Depth (km)	Mw	records	events		
1	04.03.1977	45.77	26.76	94	7.4	2	1977		
2	30.08.1986	45.52	26.49	131.4	7.1	85	1986		
3	30.05.1990	45.83	26.89	90.9	6.9	108	1990-1		
4	31.05.1990	45.85	26.91	86.9	6.4	66	1990-2		
5	27.10.2004	45.84	26.63	105.4	6.0	110	2004		

The study of the ground motions from category B is not the purpose of this paper, but at first glance the different behaviour can be explained by local site conditions, topography, directivity and path attenuation. Practically type I and II exceptions have the same two-segment pattern as category A, but with greater or lesser percentage of energy for the abrupt segment. Type III exceptions (containing 120 horizontal components of ground motions) is most likely influenced by local site conditions and in SMSIM simulations one does not need a different shaping window from that used for category A if one uses a nonlinear analysis program (e.g. DEEPSOIL - Hashash et al. 2016) for accounting the superficial soil layers behaviour; the interruptions of the abrupt segment show nonlinear soil behaviour and loose of energy in the process, and with a proper bedrock motion (that can be obtained with stochastic simulations) and a well described profile layer, the changes will be simulated through the analysis of the nonlinear local site conditions. Type IV exceptions can be simulated with SMSIM implemented shaping window.

For the accelerograms assigned to the function category (A) the statistical descriptors were determined for each earthquake separately as well as for all the five earthquakes analyzed together, as can be seen in Fig. 3. The similar behavior of energy release can be observed: overall, there is a sudden release of energy up to about 50% of the total energy and a subsequent slow release. It can also be observed that the ground motions recorded during the 1990-2 earthquake have a 60%

sudden release rate (the difference can be explained due to the different source mechanism that this earthquake had).

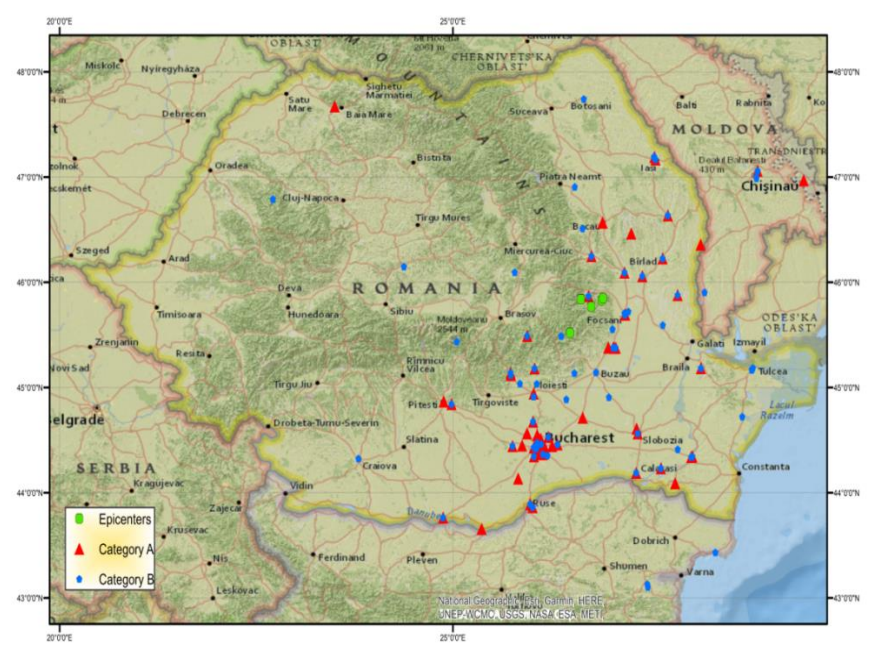


Figure 9. The map with the locations of the seismic stations of the analysed recorded ground motions produced by Vrancea (Romania) intermediate-depth earthquakes on March 4<sup>th</sup> 1977, August 30<sup>th</sup> 1986, May 30<sup>th</sup> and May 31<sup>st</sup> 1990, October 27<sup>th</sup> 2004 and the locations of the epicentres of the earthquakes. The green circles are the epicentres of the earthquakes, the red triangles are the stations where category A horizontal components were recorded, blue circles are the stations where category B horizontal components were recorded (Coţovanu & Vacareanu, 2020)

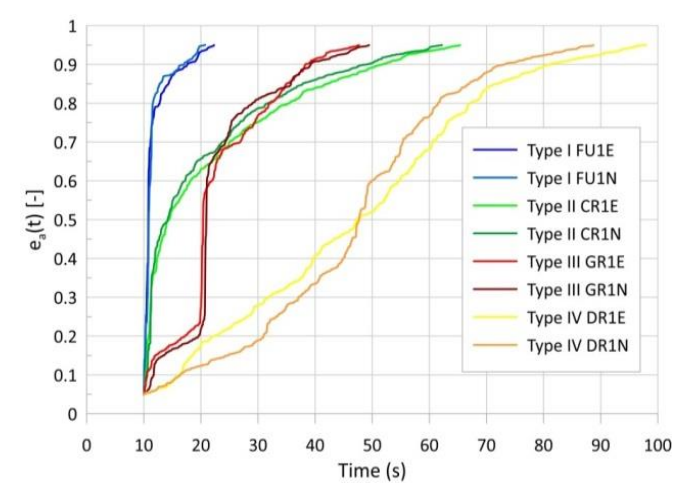


Figure 10. Examples of cumulative normalized energies from category B - exceptions; the examples are for the recorded ground motions in direction EW (E) and NS (N) of October 27th 2004 Vrancea earthquake at the stations Fulga (FU1E, FU1N; 44.888°N, 26.442°E), Craiova (CR1E, CR1N; 44.325°N, 23.800°E), Greabanul (GR1E, GR1N; 45.380°N, 26.975°E) and Draganului Valley (DR1E, DR1N; 46.792°N, 22.711°E). e<sub>a</sub>(t) is the cumulative normalized energy (Cotovanu & Vacareanu, 2020)

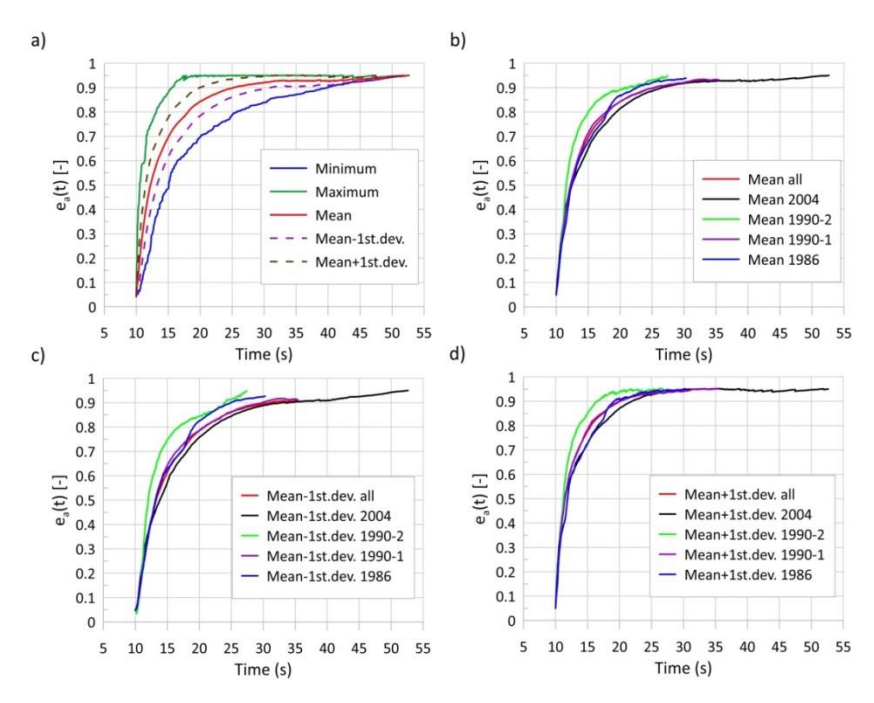


Figure 11. Statistical descriptors for the recordings from category A: a – mean values, mean minus/plus one standard deviation, maximum and minimum values for the cumulative energies of all the recordings from the earthquakes included in function category (March  $4^{th}$  1977, August  $30^{th}$  1986, May  $30^{th}$  and May  $31^{st}$  1990, October  $27^{th}$  2004); b, c, d - comparison between the mean values, mean minus one standard deviation, respectively mean plus one standard deviation of the cumulative energy of the recordings included in the category function determined for each earthquake separately as well as for all the five earthquakes together.  $e_a(t)$  is the cumulative normalized energy (Coţovanu & Vacareanu, 2020)

## 3.3. The mathematical model of the shaping window implemented in SMSIM and EXSIM. Determining the window parameters

### 3.3.1. The mathematical model of the shaping window implemented in SMSIM and EXSIM

The first steps of the time series simulations implemented in SMSIM imply generating a Gaussian or a white noise corresponding to the duration of the seismic motion and shaping it with a box or an exponential window function. When using the exponential window the duration of the motion  $T_d$  (determined as the sum of source and path durations) is extended through a factor  $f_{t_b}$  and a factor  $f_{textnd}$  so that the window does not interfere with the duration determined based on physical characteristics.

For capturing the pulse-type behaviour specific to ground motions generated by Vrancea intermediate-depth earthquakes, in the simulations the exponential window was used. The window's form was proposed by Boore (2003) after Saragoni and Hart (1974):

$$w(t, \epsilon, \eta, t_{\eta}) = a \left(\frac{t}{t_{\eta}}\right)^{b} \exp\left[-c \frac{t}{t_{\eta}}\right], \text{ where}$$
 (2)

$$a = (\exp(1)/\epsilon)^{b} \tag{3}$$

$$b = -\epsilon \ln \eta \cdot [1 + \epsilon (\ln \epsilon - 1)]^{-1} \tag{4}$$

$$c = b/\epsilon \tag{5}$$

$$t_{\eta} = f_{T_g} \cdot T_d \tag{6}$$

where: t-time; a, b, c-shape parameters;  $t_{\eta}-normalization$  time;  $\epsilon-the$  normalized time where the window has a peak value of unity;  $\eta-the$  value of the window when the normalized time is 1;  $T_d-source$  and path duration;  $f_{T_g}=f_{t_b}-a$  factor that extends the duration of the seismic motion and changes the shape of the window,  $f_{t_b}$  is the notation used in the programs

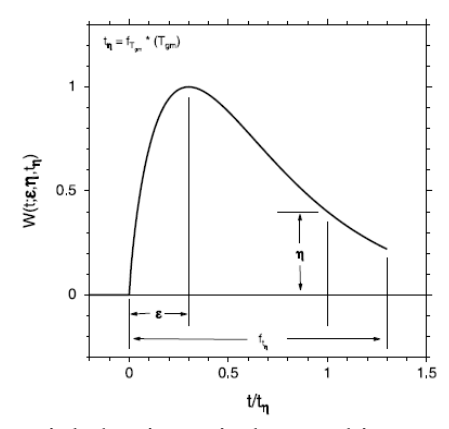


Figure 12. The exponential shaping window and its parameters (Boore, 2003)

In the paper of Saragoni and Hart (1974), the authors proposed an accelerogram simulation method that involves modeling the variation of the mean square acceleration using a time-based envelope function. The variation of the frequency content in their method was captured using three regions with unique and uni-modal power spectral densities. They demonstrate that the envelope modeling function  $\psi(t)$  is derived from the expected mean square acceleration  $E[a^2(t)]$ :

$$E[a^2(t)] = \psi^2(t) \tag{7}$$

Using the postulated form for the expected mean square acceleration:

$$E[a^2(t)] = \beta t^{\gamma} e^{-\alpha t} \tag{8}$$

the shape of the envelope function for modeling the amplitude variation over time being:

$$\psi(t) = \sqrt{\beta} t^{0.5\gamma} e^{-0.5\alpha t} \text{ (form used in SMSIM and EXSIM)}$$
 (9)

where:  $\beta$  – intensity parameter;  $\alpha$ ,  $\gamma$  – shape characterization parameters; a(t) – the time-history of ground motion acceleration

The expected energy function of the acceleration is defined by:

$$E[W_a(t)] \equiv \int_0^t E[a^2(\tau)] d\tau \tag{10}$$

$$E[W_a(t)] = \int_0^t \beta \tau^{\gamma} e^{-\alpha \tau} d\tau = \beta P(\gamma + 1, \alpha t) \frac{\Gamma(\gamma + 1)}{\alpha^{\gamma + 1}} \text{ unde}$$
 (11)

$$P(a,x) = \frac{1}{\Gamma(a)} \int_0^x t^{a-1} e^{-t} dt$$
 (12)

P(a, x) - incomplete gamma function;  $\Gamma(a)$  - gamma function.

The method for determining the parameters of the envelope-function involves finding the most suitable curve for describing the average energy through interpolation.

The window function parameters were determined for the mean, mean plus one standard deviation and mean minus one standard deviation of the cumulative normalized energies of all the records included in the A category. The determination was made using the curve-fitting process from Matlab for the imposed function  $\beta P(\gamma+1,\alpha t)\frac{\Gamma(\gamma+1)}{\alpha^{\gamma+1}}$  that is the expected energy function of the acceleration defined by Saragoni & Hart (1974). The correlation squared values (R-sq) between the analyzed cumulative energies and the predicted functions were of values greater than 99.60% and the root mean squared errors (RMSE) were less than 0.011 for all three cases, indicating a very good fit.

With the obtained parameters (see Table 6), the window functions  $\psi(t)$  are calculated after Saragoni and Hart (1974) (Figure 13) and then transformed in the required format  $w(t, \epsilon, \eta, t_{\eta})$  for SMSIM (Boore, 2003). As it can be observed, from Figure 14, the window implemented in SMSIM, recalculated for the program's requirements with  $\epsilon$  and  $\eta$  parameters (Table 7), does not retain the same shape.  $\epsilon$  and  $\eta$  were determined according to the definitions from Boore (2003),  $\epsilon$  being the normalized time where the window has a peak with value of unity and  $\eta$  is the value of the window where the normalized time is 1 (Table 7 contains the algorithm). The inverse calculation of  $\epsilon$  and  $\eta$  (from a, b, c to  $\epsilon$  and  $\eta$ ) cannot be achieved because  $\epsilon$  would be negative and the formula for b implemented in the program has a logarithm in  $\epsilon$  that would not be defined.

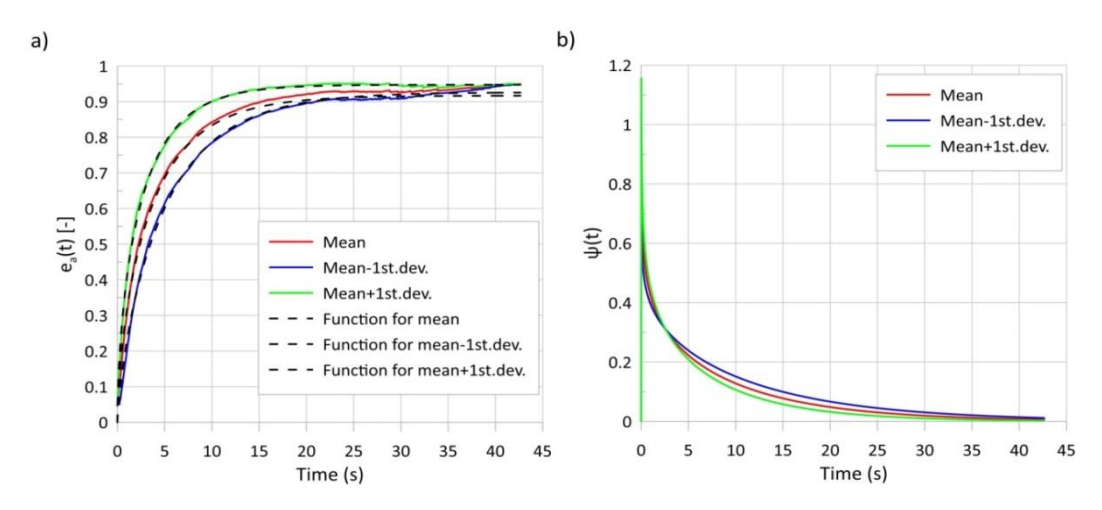


Figure 13. a Comparison between the analysed cumulative energies and the predicted functions; b Window functions  $\psi(t)$  for modeling the amplitude variation over time (Coţovanu & Vacareanu, 2020)

Table 6. Parameter values resulted from curve-fitting (Cotovanu & Vacareanu, 2020)

	Maan with 05% confidence			Mean-1 standard deviation			Mean+1 standard deviation		
	Mean with 95% confidence bounds		with 95% confidence bounds			with 95% confidence bounds			
-									
		best fit			best fit			best fit	
α	0.1627	0.1693	0.1651	0.1443	0.146	0.1476	0.208	0.2099	0.2114
β	0.2099	0.2106	0.2113	0.1797	0.1804	0.181	0.2481	0.2491	0.2501
γ	-0.3778	-0.3744	-0.371	-0.2685	-0.2624	-0.2563	-0.4333	-0.4303	-0.4273

Table 7. Parameter values resulted from curve-fitting and transformed in the required SMSIM format for the mean cumulative energy (Cotovanu & Vacareanu, 2020)

Parameters resulted from curve- fitting for the form proposed by Saragoni and Hart (1974) $\psi(t) = \sqrt{\beta} t^{0,5\gamma} e^{-0,5\alpha t}$		Transformed param Boore (2003) funct - equation (	Recalculated parameters after $\varepsilon$ and $\eta$ - equations (3), (4), (5) $w(t, \varepsilon, \eta, t_{\eta})$		
α	0.1693	$a = \sqrt{\beta} / \psi(\mathrm{d}t/t_{\eta})$	0.2440	a	1.004687
β	0.2106	$b = 0.5\gamma$	-0.1872	b	0.000803
γ	-0.3744	$c = 0.5\alpha$	0.08465	c	1.501765
$f_{t_b}$ (parameter for time normalizing and duration extending)	1.0	$\eta = \psi(1)/\psi(\mathrm{d}t/t_{\eta})$	0.22426	$t_{\eta} = T_{D}$ $T_{D} = sou$	· f <sub>Tg</sub> erce+path
$f_{t_{ext}}$ (parameter for extending the duration for window application)	5.0	$\varepsilon = \frac{dt}{t_{\eta}}$	0.00053	$T_D = source + path$ duration $f_{T_g} = f_{t_b}$ dt - time step	

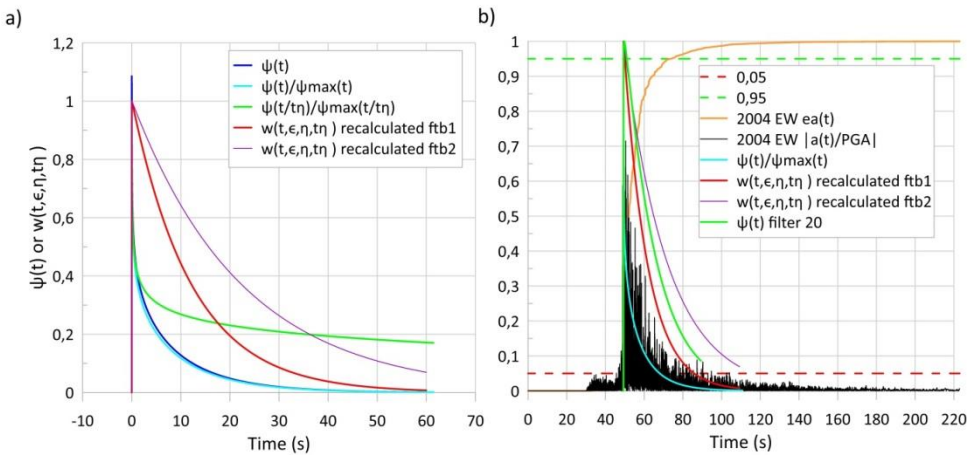


Figure 14. a Comparison between window function  $\psi(t)$ , window function scaled to  $1 \psi(t)/\psi$  window function in normalized time scaled to  $1 \psi(t/t_\eta)/\psi$  max $(t/t_\eta)$  and window function recalculated with  $\epsilon$  and  $\eta$  for the mean cumulative energy of all five earthquakes; b Comparison between the normalized accelerogram and cumulative energy of the ground motion recorded at the INCERC station (EW direction) during the 2004 Vrancea earthquake and the normalized window function  $\psi(t)/\psi$ max(t) in the form proposed after Saragoni and Hart (1974), recalculated  $w(t, \epsilon, \eta, t_\eta)$  with  $\epsilon$  and  $\eta$  after Boore (2003) with the extending factor  $f_{t_b}$  1 and 2 and the window 20 (Fig. 1) used in Chapter 2 (Coţovanu & Vacareanu, 2020)

As the time approaches zero, the window function  $\psi(t)$  (equation 8) approaches asymptotically to infinity so the scaling to 1 and the  $\epsilon$  parameter depends on the chosen time step (the origin of functions from the figures were imposed in 0 for illustrative purposes). Also as it can be seen in Figure 14a, the time normalized function changes dramatically. In Figure 14b it can be noticed that the window functions  $\psi(t)$  calculated after Saragoni and Hart (1974) and scaled to 1 would provide a good fit to the imaginary line going through the peaks of the accelerogram, if the window was to be translated both on the x and y axes.

The recalculated window function describes (Fig. 8), according to the chosen  $f_{t_b}$ , larger or smaller amplitudes of the noise compared to those described by window 20 that was used in Chapter 2, but the decrease of the amplitudes is still described in a progressing manner ( $f_{t_b} = 2$  is the value used by Boore 2003). As it may be observed, the determined parameters of the mean do not improve the shape used as the better fit in the above-mentioned chapter (for comparison purposes simulations with the "mean" one-piece windows are made in section 3.5).

## 3.4. Defining a two intervals shaping window that can describe the specific energy release of ground motions generated by Vrancea intermediate-depth strong earthquakes

### 3.4.1. Continuity and derivability issues in modeling the energy release shaping window

Given that it is proposed to use a window with several intervals, the issue of its continuity and derivability will be analysed. The shape of the envelope function will be preserved as defined by Saragoni and Hart (1974), but two sets of parameters will be defined, as follows:

$$\psi(t) = \begin{cases} \sqrt{\beta_1} t^{0.5\gamma_1} e^{-0.5\alpha_1 t} & t \in (0, t_0) \\ \sqrt{\beta_2} t^{0.5\gamma_2} e^{-0.5\alpha_2 t} & t \in [t_0, t_{final}) \end{cases}$$
(13)

$$E[W_a(t)] = \begin{cases} \beta_1 P(\gamma_1 + 1, \alpha_1 t) \frac{\Gamma(\gamma_1 + 1)}{\alpha_1 \gamma_1 + 1} & t \in (0, t_0) \\ \beta_2 P(\gamma_2 + 1, \alpha_2 t) \frac{\Gamma(\gamma_2 + 1)}{\alpha_2 \gamma_2 + 1} & t \in [t_0, t_{final}) \end{cases}$$
(14)

### Conditions:

- 1. The expected energy function must be continuous in t<sub>0</sub>
- 2. The expected energy function must be derivable in  $t_0$
- 3. If the window follows the form presented by Boore (2003) the window has a local maximum in the first interval

Because  $t_0$  will be defined as a variable parameter depending on the database used to determine the parameters, for the matter of studying the problem of continuity and derivability,  $t_0$  is considered arbitrary.

Parameters for two intervals 0 - 10 s and 8 s -  $t_{final}$  are determined using the curve-fitting process in Matlab for the imposed function  $\beta P(\gamma + 1, \alpha t) \frac{\Gamma(\gamma + 1)}{\alpha^{\gamma + 1}}$ . The interpolation intervals intersect on the portion 8-10 s to achieve a smooth transition between the two functions.

The function thus defined is neither derivable nor continuous at any point from  $t \in (8, 10)$ . Even if the parameters could be slightly changed aiming to find a point  $t_0$  of continuity, the function cannot be derivable at that point because by defining the shaping window on two intervals the purpose was to dramatically change the slope of the expected energy function. For this reason, a three-interval envelope function was defined, using a polynomial linking function.

As for the third condition, the second order derivative of the first interval of the expected energy function  $E''[W_a(t)]$  strives asymptotically to  $-\infty$  when  $t \to 0$  and to 0 when  $t \to \infty$ , so there is no maximum point in the first interval function. This means that the first point of the window

depend on the time step chosen for the simulation and the window will need scaling in order to achieve a maximum equal to unity.

For the three-interval envelope function, for the first and third intervals the previous form of energy definition was considered, and for the second interval a 3rd degree polynomial function was used as follows:

$$\psi(t) = \begin{cases} \sqrt{\beta_1} t^{0.5\gamma_1} e^{-0.5\alpha_1 t} & t \in (0, t_0) \\ \sqrt{3p_1 t^2 + 2p_2 t + p_3} & t \in [t_0, t_1) \\ \sqrt{\beta_2} t^{0.5\gamma_2} e^{-0.5\alpha_2 t} & t \in [t_1, t_{final}) \end{cases}$$
(15)

$$E[W_{a}(t)] = \begin{cases} \beta_{1}P(\gamma_{1}+1,\alpha_{1}t)\frac{\Gamma(\gamma_{1}+1)}{\alpha_{1}\gamma_{1}+1} & t \in (0,t_{0}) \\ p_{1}t^{3} + p_{2}t^{2} + p_{3}t + p_{4} & t \in [t_{0},t_{1}) \\ \beta_{2}P(\gamma_{2}+1,\alpha_{2}t)\frac{\Gamma(\gamma_{2}+1)}{\alpha_{2}\gamma_{2}+1} & t \in [t_{1},t_{final}) \end{cases}$$
(16)

For the first and third branches the parameters were determined using the curve-fitting process for the intervals 0-8 s and 12 s -  $t_{final}$ . Those from the polynomial branch (8-12s) resulted from the system of equations made with the continuity and the derivability conditions. Defining the function as mentioned above, the imposed conditions are met, but when normalized according to the method implemented in SMSIM and EXSIM, the function thus defined loses its continuity. However, by scaling the function to reach a unit peak the continuity is preserved. Because  $t_0$  and  $t_1$  are variable parameters, to verify the function's continuity and derivability for another time intervals, the values  $t_0 = 12s$  and  $t_1 = 16s$  were chosen. Both the continuity and the derivability of the function were lost; even more for a time greater than 15.75 s the window-function becomes negative

The time domain stochastic simulations are performed with discrete variables. Modeling the generated white noise with a shaping window that is not continuous assumes that in  $t_0$  the function will not coincide at limit. Because the multiplication of the white noise with the window is performed in a discrete domain, the noise has no values in the  $t_0$  and  $t_0$  + dt interval; therefore the simulation will not be influenced.

### 3.4.2. Defining the window function's intervals

To determine the intervals for defining the two branches of the window, we seek the point  $(t_0)$  where a more sudden change in the tangent to the expected mean energies is noticed. Three hypotheses were considered: the last slope greater than 0.1, the last slope greater than 0.05 and the first negative slope (negative slopes occur because the cumulative expected energies are averaged and the mean values might decrease; obviously, this behaviour will not be found in reality at the cumulative energy of a single accelerogram).

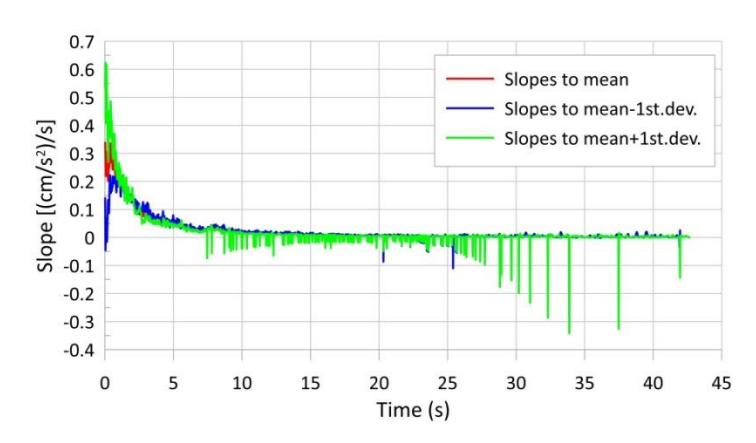


Figure 15. The evolution of the slopes to the mean, mean plus one standard deviation and mean minus one standard deviation of the cumulative normalized energy curves of the five analysed earthquakes (Cotovanu & Vacareanu, 2020)

Table 8. The point in time (t<sub>0</sub>) and in cumulative normalized energy where a more sudden change in the tangent to the expected energies is noticed for the three cases: Case I - the last slope greater than 0.1, Case II - the last slope greater than 0.05 and Case III - the first negative slope (Cotovanu & Vacareanu, 2020)

negative stope (	Coțo vana &	v acarcana, 2020)			
Case I	Time (s)	$e_a(t)$ [-]	Last slope >0.1		
Mean	2.50	0.528	0.107		
Mean+ 1 standard deviation	2.54	0.636	0.114		
Mean-1 standard deviation	3.18	0.494	0.102		
Case II	Time (s)	$e_a(t)$ [-]	Last slope >0.05		
Mean	5.42	0.716	0.052		
Mean+ 1 standard deviation.	5.60	0.803	0.056		
Mean-1 standard deviation	5.44	0.639	0.055		
Case III	Time (s)	$e_a(t)$ [-]	First slope <0		
Mean	7.46	0.779	-0.025		
Mean+ 1 standard deviation	7.46	0.850	-0.074		
Mean-1 standard deviation.	12.30	0.825	-0.011		

## 3.4.3. Defining the new envelope function after the model proposed by Sharagoni and Hart (1974)

The shape of the envelope function will be preserved as defined by Saragoni and Hart (1974), but two sets of parameters will be defined, as follows:

$$\psi(t) = \begin{cases} \sqrt{\beta_1} t^{0.5\gamma_1} e^{-0.5\alpha_1 t} & t \in (0, t_0) \\ \sqrt{\beta_2} t^{0.5\gamma_2} e^{-0.5\alpha_2 t} & t \in [t_0, t_{final}) \end{cases}$$
(17)

$$E[W_a(t)] = \begin{cases} \beta_1 P(\gamma_1 + 1, \alpha_1 t) \frac{\Gamma(\gamma_1 + 1)}{\alpha_1^{\gamma_1 + 1}} & t \in (0, t_0) \\ \beta_2 P(\gamma_2 + 1, \alpha_2 t) \frac{\Gamma(\gamma_2 + 1)}{\alpha_2^{\gamma_2 + 1}} & t \in [t_0, t_{final}) \end{cases}$$
(18)

$$P(a,x) = \frac{1}{\Gamma(a)} \int_0^x t^{a-1} e^{-t} dt$$
 (19)

P(a,x) - incomplete gamma function;  $\Gamma(a)$  - gamma function;  $\alpha_1,\beta_1,\gamma_1,\alpha_2,\beta_2,\gamma_2$  - shape characterization parameters;  $t_0$  - the time point where a more sudden change in the tangent to the

expected energies is noticed;  $t_{final}$  – the total duration of simulation determined by SMSIM after the source and path durations and the extension parameters.

Window-function's parameters were determined using MATLAB's curve-fitting application for the imposed function  $\beta P(\gamma+1,\alpha t)\frac{\Gamma(\gamma+1)}{\alpha^{\gamma+1}}$  for each interval and each case (Tables 6). The statistical measures of the curve-fitting process indicated a very good fit (the square of the correlations are greater than 98.80% and root mean squared error is less than 0.0082).

Table 9.	Parameter values	resulted from curv	e-fitting (Cotova	ınu & Vacareanu, 202	(0)
I dolo ).	i didilictoi valaco	1 Counted II offi Cui v	c municipal corone	ma ee vacareama, 202	, ,

					<u> </u>	,				
	Case I				Case II			Case III		
For mean cumulative	t0=2.50s with 95% confidence			t0=5.46s	t0=5.46s with 95% confidence			t0=7.46s with 95% confidence		
energy case	bounds				bounds			bounds		
		best fit			best fit			best fit		
$\alpha_1$ (1 <sup>st</sup> interval)	0.1241	0.1892	0.2544	0.2832	0.3941	0.305	0.257	0.2634	0.2699	
$\beta_1$ (1 <sup>st</sup> interval)	0.2243	0.243	0.2618	0.2641	0.2691	0.2741	0.2531	0.2562	0.2593	
$\gamma_1$ (1 <sup>st</sup> interval)	-0.2948	-0.2604	-0.2265	-0.2364	-0.2245	-0.2129	-0.2596	-0.2511	-0.2427	
$\alpha_2$ (2 <sup>nd</sup> interval)	0.1437	0.1448	0.1459	0.1433	0.1451	0.1469	0.1454	0.1481	0.1509	
$\beta_2$ (2 <sup>nd</sup> interval)	0.1995	0.2002	0.2008	0.1993	0.2003	0.2014	0.2005	0.2019	0.2033	
$\gamma_2$ (2 <sup>nd</sup> interval)	-0.4458	-0.4421	-0.4384	-0.4482	-0.4409	-0.4335	-0.4387	-0.4261	-0.4135	

### 3.4.4. Redefining parameters for the time normalized form proposed after Boore (2003)

As it can be seen in Figure 14 the time normalized window proposed by Saragoni and Hart significantly loses its form and for using it with normalized time one should redefine the parameters according to Boore (2003). For this purpose the algorithm must be discussed because the second branch of the window depends on the parameters from the first branch. So if the window is rewritten, transformations should be done to retain the difference between the values of the function's branches at the point  $t_0$  and retain the same normalization to the first maximum of the function. When the maximum of the first branch is at the first time step, the algorithm for calculating the parameters and the window in the form proposed after Boore (2003) are:

$$w(t, \epsilon, \eta, t_{\eta}) = \begin{cases} a_1 \left(\frac{t}{t_{\eta}}\right)^{b_1} \exp\left[-c_1 \frac{t}{t_{\eta}}\right] & t \in (0, t_0) \\ a_2 \left(\frac{t}{t_{\eta}}\right)^{b_2} \exp\left[-c_2 \frac{t}{t_{\eta}}\right] & t \in [t_0, t_{final}) \end{cases}, \text{ where}$$

$$(20)$$

$$a_1 = (\exp(1)/\epsilon_1)^{b_1}$$
 (21)

$$b_1 = -\epsilon_1 \ln \eta_1 \cdot [1 + \epsilon_1 (\ln \epsilon_1 - 1)]^{-1}$$
(22)

$$c_1 = b_1/\epsilon_1 \tag{23}$$

$$a_2 = \frac{1}{\left(\frac{t_0}{t_\eta}\right)^{b_2} \exp\left[-c_2 \frac{t_0}{t_\eta}\right]} \cdot \frac{\psi_2\left(\frac{t_0}{t_\eta}\right)}{\psi_1\left(\frac{dt}{t_\eta}\right)}$$
(24)

$$b_2 = -\epsilon_2 \ln \eta_2 \cdot [1 + \epsilon_2 (\ln \epsilon_2 - 1)]^{-1}$$
(25)

$$c_2 = b_2/\epsilon_2 \tag{26}$$

$$\eta_1 = \psi_1(1)/\psi_1(dt/t_n)$$
 (27)

$$\eta_2 = \psi_2(1)/\psi_2(dt/t_{\eta})$$
(28)

$$\varepsilon_{1,2} = \frac{\mathrm{dt}}{\mathsf{t_n}} \tag{29}$$

where  $t_{\eta} = f_{T_g} \cdot T_d$  – normalization time;  $a_1, b_1, c_1, a_2, b_2, c_2$  – shape characterization parameters;  $\epsilon_{1,}\epsilon_{2}$  - the normalized time where each branch of the window  $\psi(t)$  has a peak value of unity;  $\eta_{1,}\eta_{2}$  – the value of each branch of the window when the normalized time is 1;  $\psi_{1}(t)$  – first branch of the

window  $\psi(t)$ , for  $t \in (0, t_0)$ ;  $\psi_2(t)$  – second branch of the window  $\psi(t)$ , for  $t \in (t_0, t_{\text{final}})$ ;  $f_{\text{Tg}} = f_{t_b}$  – a factor that extends the duration of the seismic motion and changes the shape of the window,  $f_{t_b}$  is the notation used in SMSIM; the transformation algorithm is valid for the case where the maximum of the first branch is at the first time step; if the maximum is in the range  $t \in (dt, t_0)$  the normalization will be done with that maximum

The shape of the window in both forms can be seen in Figure 16. Because the shape of the function proposed by Boore (2003) is influenced by the normalization time, by writing the window with two branches one can use different extension factors  $f_{t_b}$  for the branches. For the windows presented in Figure 16 and used in simulations, the first interval has  $f_{t_b} = 1.00$ , and the second interval  $f_{t_b} = 2.25$ .

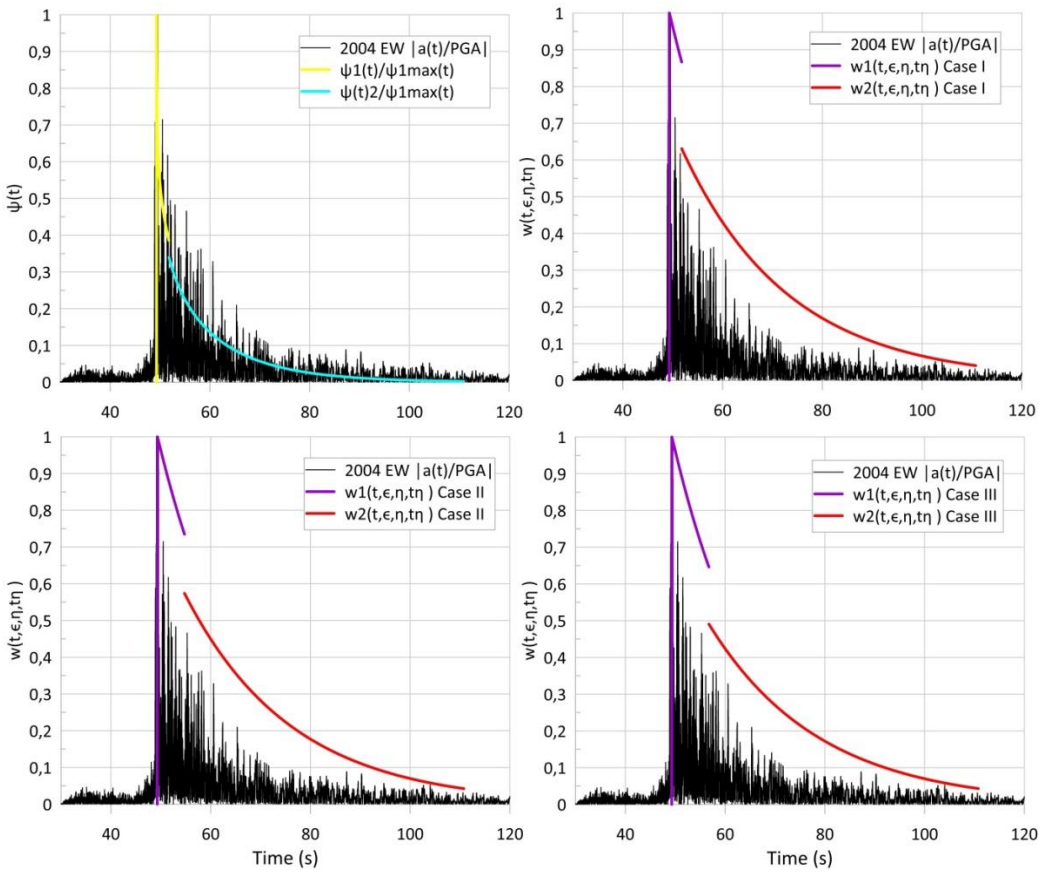


Figure 16. Comparisons between the normalized accelerogram of the ground motion recorded at the INCERC station (EW direction) during the 2004 Vrancea earthquake and the two-interval window function in the form proposed after Saragoni and Hart (1974) scaled to 1 ( $\psi$ 1(t)/ $\psi$ 1max(t) – first interval,  $\psi$ 2(t)/ $\psi$ 1max(t) – second interval), and the recalculated two-interval windows for every defined case (w1(t,  $\epsilon$ ,  $\eta$ , t<sub> $\eta$ </sub>) – first interval, w2(t,  $\epsilon$ ,  $\eta$ , t<sub> $\eta$ </sub>) – second interval) (Cotovanu & Vacareanu, 2020)

### 3.5. Simulations in SMSIM using the newly defined window function

For checking the window-function defined above, 400 simulations were made for each case using the modified SMSIM set of programs for Vrancea (Romania) intermediate-depth earthquake produced on October 27th 2004, INCERC station (the analysed accelerogram is the one with the closest peak ground acceleration PGA to the mean PGA of the simulations). The code of SMSIM

was modified so that the new window can be implemented. Two types of simulation were made: one with the exact parameters defined above for the form proposed after Sargoni and Hart (1974) and one with redefined parameters for the time-normalized form. For comparison purposes, simulations with the one-piece "mean" window were made. For the second branch of the new function for each case and for one of the "mean" one-piece window the extension factor  $f_{t_b}$  was considered 2.25 and for the first branch and the other one-piece window it was considered 1. The parameters considered in the simulations are those of Chapter 2 with the change of the path duration to the initial value of 0.0868 and the scattering modified as  $R^{(-0.45)}$ .

It can be observed from Figure 17 and Table 10 that the one-piece window with  $f_{t_b}=1$  and the two-interval function in the form of Saragoni and Hart describe a similar release of energy. By recalculating the parameters of the two-interval window using the  $\varepsilon$  and  $\eta$  as defined above, a suitable approximation of the significant duration, root mean square and peak ground acceleration is obtained. Comparing these results to the simulation made with the one-piece window with  $f_{t_b}=2.25$  one may observe that by its incapacity to describe the first abrupt segment, the energy is distributed progressively to a longer significant duration that produces a lower peak value. All the two-interval cases describe the first abrupt interval and the second progressive interval, case III having a little too long first segment. Simulations for cases I and II are illustrated in Figure 18. It can be observed that the first strong portion is captured and that the peaks of the tail are significantly lower than those from the first portion.

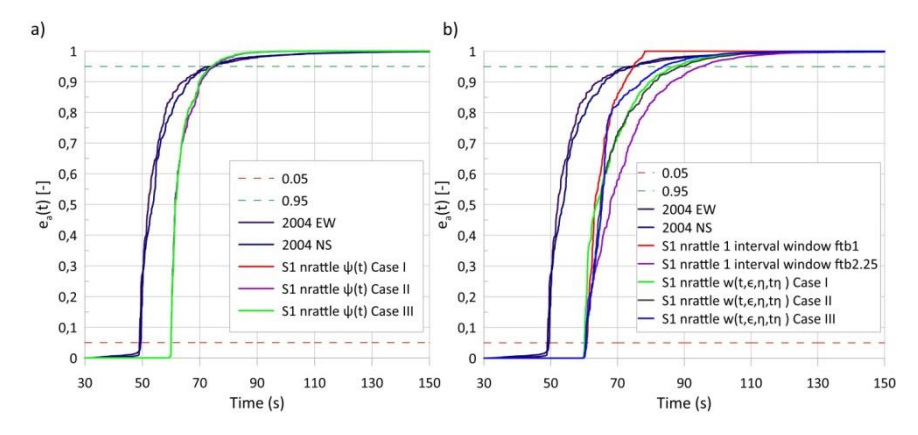


Figure 17. a Comparison between the simulated cumulative energies with the newly defined window function and those of the earthquake of October 27<sup>th</sup> 2004, INCERC station; b Comparison between the simulated cumulative energies with the new window function recalculated for the form proposed by Boore (2003) and those of the earthquake of October 27<sup>th</sup> 2004, INCERC station (Cotovanu & Vacareanu, 2020)

A problem still remains, the root mean square accelerations are still a little higher, but this may be explained by the contribution of the P waves in the recorded accelerograms that is not accounted for in the simulations (the simulations being made only for S waves). Also, further research should be done to establish why the window with the original values of parameters determined with Matlab with such good fit indicators cannot estimate the proper energy release and why by recalculating them the expected result is obtained, but it should be mentioned that in the first form of the program (Boore, 1983) the window was not normalized with time, the normalization being added later.

In the case of Vrancea ground motion simulations the shaping window has an important contribution because, practically, the energy described by the spectrum of the motion - determined considering the physical parameters - is distributed in time in accordance with the shape of the noise, and if the noise has an uniform peak distribution the simulations have more peaks with values appropriate to the PGA. That means that the energy would be approximately uniformly distributed over the duration, and depending on the length of the duration the peaks would have higher or lower values. By shaping the noise properly, the energy is guided to fill more the first segment of the motion and less the long descending tail.

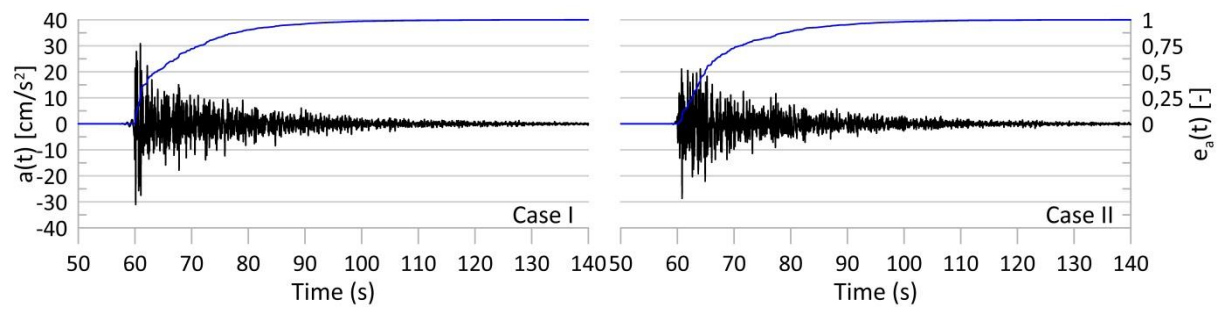


Figure 18. Examples of simulated accelerograms obtained using the two-interval window for the defined cases I and II for the characteristics of the ground motions produced by October 27<sup>th</sup> 2004 Vrancea earthquake recorded at the INCERC (Cotovanu & Vacareanu, 2020)

Table 10. Characteristics of simulated ground motions made using the modified with the newly defined window function SMSIM (Cotovanu & Vacareanu, 2020)

Type of simulation using SMSIM	PGA (cm/s <sup>2</sup> )	Significant duration (s)	Root mean square (cm/s <sup>2</sup> )
S1 mean parameters one interval window $f_{t_b} = 1$	35.1	14.03	8.1
S1 mean parameters one interval window $f_{t_b} = 2.25$	23.0	34.73	4.8
S1 nrattle window 1 <sup>st</sup> case	47.0	7.61	10.0
S1 nrattle window 2 <sup>nd</sup> case	45.3	7.95	9.7
S1 nrattle window 3 <sup>rd</sup> case	46.6	7.62	9.8
S1 nrattle window recalculated, 1 <sup>st</sup> case	31.0	26.91	5.6
S1 nrattle window recalculated, 2 <sup>nd</sup> case	28.7	28.02	5.5
S1 nrattle window recalculated, 3 <sup>rd</sup> case	29.1	23.25	5.9
INCERC 2004 EW	29.7	24.80	4.4
INCERC 2004 NS	30.0	25.65	5.0

### 3.6. Conclusions

This chapter focused on defining a shaping window, for the time series stochastic simulation method implemented in the program SMSIM, that can depict the energy release observed at ground motions generated by Vrancea intermediate-depth earthquakes.

For this purpose a number of 371 horizontal components of ground motions recorded at different seismic stations during March 4th 1977, August 30th 1986, May 30th and May 31st 1990, October 27th 2004 earthquakes were analysed. Five types of energy release patterns (behaviours) were defined as: category A (typical pattern for almost half of the records) where the evolution in time of the cumulative energies has a first abrupt segment where, on average, approximately 50% of

the energy is released in the first 1.5-3 s of strong motion, and then a second segment of 20-40 s where the energy is slowly released, and category B or exceptions category with type I, II, III and IV exceptions. For A category ground motions the statistical descriptors were determined for each earthquake separately as well as for all the five earthquakes together.

It was shown that the exponential window implemented in SMSIM is not able to capture the specific form of the energy release of ground motions generated by Vrancea intermediate-depth earthquakes, overestimating the root mean square accelerations and underestimating the significant duration or vice versa, according to the chosen extension factor.

A suitable two-interval window for modeling the shape of the generated white noise used in stochastic simulations was defined and implemented in SMSIM. For the newly defined two-interval window function an algorithm for calculating the parameters was described, and for the mean release of energy of the ground motions with typical pattern (category A) parameters were determined. More appropriate ground motion simulations were obtained by using the two-interval function for describing the Vrancea specific release of energy. With the procedure described in the paper one can easily define parameters for the two-interval window function for specific Vrancea earthquakes.

Further research should be conducted regarding the other parameters that influence the ground motion simulation for a better fitting. Duration parameters depend mainly on the source and path duration. Taking into account directivity for example would decrease the source duration, and amplitude parameters will change if other attenuation functions for path would be used. For stochastic simulations all the parameters mentioned in introduction influence the results, but in this paper only the shaping window was analysed and a more appropriate form was defined for it. A more precise set of parameters for the window could be found after including the ground motions generated by Vrancea intermediate-depth earthquakes in group types according to more complex classification rules, taking into account the source-to-site distance, directivity, topography, path attenuation and local site conditions. Also when generating ground motions for recorded accelerograms, in order to obtain better results, one may determine specific parameters for the two-interval window function.

## 4. Defining the parameters of the seismic action used in the simulation of ground motions generated by Vrancea intermediate-depth seismic source

### 4.1. Introduction

The time series stochastic simulation method implies generating of a white or a Gaussian noise and modifying it with the specific characteristics of the target ground motion. The spectrum of the motion with which the shaped and normalized spectrum of the noise is modified encompasses the characteristics of the source, of the path travelled by the waves and the changes given by the local site conditions. The stochastic method is a complex simulation method because it tries to capture as much as possible the phenomena that produce and modify the seismic waves. The success of the method depends on establishing the characteristic parameters. If for the seismic motions produced in a certain location by a past earthquake the characteristics determination is more accessible, the estimation of the parameters for a hypothetical scenario becomes more difficult due to the multitude of variables and associated uncertainties.

Thus, for characterizing the source one should estimate the locations with high probability of generating the target earthquake, the density of the material and the velocity of the waves near the hypocenter, the focal mechanism, the released energy (magnitude), the stress drop, the source duration with the directivity's influence and the source dependent radiation pattern. For characterizing the path from the source to the local site superficial layers one should define the geometrical scattering, the attenuations and the path duration. The influence of the local soil conditions is defined by the amplifications and attenuations specific to the behavior of the local soil layers (linear or nonlinear behavior, the occurrence of liquefaction phenomena, etc.).

The determination of the parameters used in the stochastic method is essential, each parameter influences the final result, and a poor estimation can lead to a less realistic simulation. This chapter aims to establish a set of parameters that can be used for various target scenarios specific to Vrancea intermediate-depth earthquakes, for various areas outside the Carpathian Arch.

The Vrancian intermediate zone is defined as a seismic nest having a stationary, but intense activity, persistent over time and isolated from the nearby seismic activity. The most known intercontinental seismic nests are Bucaramanga (Colombia) - the smallest and the most active -, Hindu Kush (Afghanistan) - the deepest - and Vrancea (Romania) (Manea, et al., 2011).

An important feature of the Vrancea region is the complex continental convergence regime, Vrancea region is in contact with the following tectonic units: in North and North-East with the East-European Platform, in East with the Scythia Platform, the Dobrogea North Orogen is in the South-East part, The Moesic Platform is in the South and South-West part and the Carpathian Orogen and Transylvanian Basin (Intra-Alpine Plate) is in the West and North-West part.

For a deeper knowledge of Vrancea regional tectonics, geodynamics, seismicity, lithospheric deformation and stress regime, over the years, a large number of geological, geodetic, geophysical, seismic, geoelectric, gravimetric, thermometric studies have been carried out and several models have been developed. In the paper "Geodynamics and intermediate-depth seismicity in Vrancea (the

south-eastern Carpathians): Current state-of-the-art", Ismail-Zadeh et al. (2012) presents the current state of the geodynamic models.

In this chapter of the thesis, comparative analyses were performed and all the parameters needed to simulate ground motion simulations generated by Vrancea intermediate-depth seismic source were defined. The analysed parameters were: locations of Vrancian intermediate earthquakes, material density and S seismic wave velocity near the hypocenter, predominant focal mechanisms, released energy (magnitude, seismic moment), corner frequency of S waves specific to source spectrum, stress drop parameter, source duration and the influences of the directivity on it, the source area, the source dependent radiation pattern, the characteristics of the propagation media crossed by the seismic waves, areas division according to the effects of the mediums travelled by the seismic wave from the source to the surface, geometrical scattering, path dependent attenuation and dispersion, the path duration, the modeling of the local site conditions for SMSIM and EXSIM, and alternative nonlinear and equivalent linear modeling.

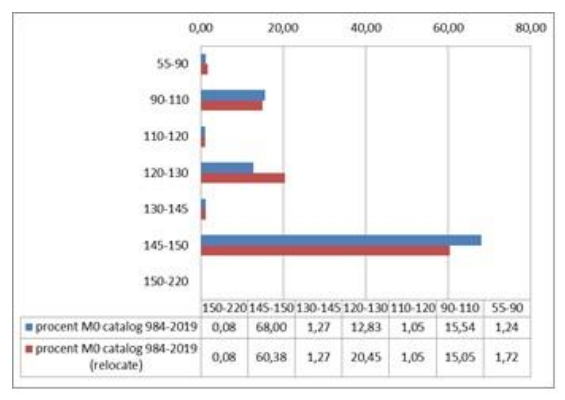
In the summary, only the parameters of the location with high potential for producing major events and the duration dependent on the are presented in detail. For these parameters special studies have been carried out because the problem of location was addressed in many studies (over 20 research papers) without reaching a uniform conclusion, and the path duration was never studied in the form needed for simulations.

### 4.2. The locations of the Vrancea intermediate-depth earthquakes

Choosing the parameters of the location of the hypocenter (latitude, longitude and depth) is probably the most important step in performing hypothetical earthquake simulations because they control the source to site distance (a small variation - relative to the dimensions of the seismic nest - significantly changes the frequency content of the simulated accelerograms), the density and the seismic wave velocity in the vicinity of the hypocenter are location dependent, the focal mechanisms register differences by depth, and the maximum possible magnitude is estimated according to the depth.

Given the fact that in the literature there are several variants of depth distribution and many proposals for estimating the intervals with potential to generate a large earthquake, an analysis of the earthquakes distribution on depth has been performed. This analysis was performed on 4 databases from the ROMPLUS catalogue (Radulian, et al., 2019): earthquakes from 984-2019, from 1940-2019 and the same time intervals with depth changes for 4 major earthquakes after the relocation calculations made by Hurukawa et al. (2008) (1940 - 124 km, 1977 - 98 km, 1986 - 135 km, 1990 - 84 km). The analysis was performed at intervals of 10 km (usual value of the accepted error) starting from a depth of 55 km, and then from 60 km (depths chosen based on the aseismicity limit of the upper part of the seismic body). For each interval the cumulative seismic moment was calculated.

Then, by intersecting the results of the two types of intervals, the energy released was obtained on irregular depths intervals that generate the largest amounts of energy (Figure 19).



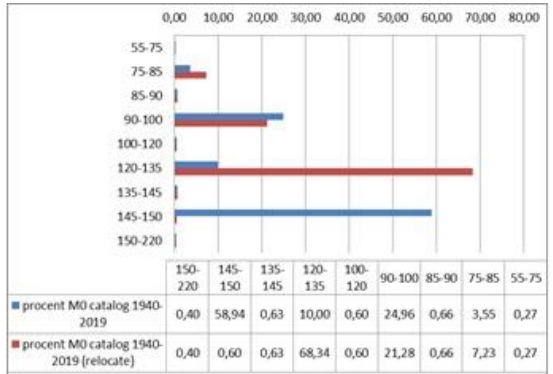


Figure 19. Percentage of seismic energy release at irregular depth intervals

The conclusions drawn from the analysis are:

- A large number of earthquakes on an interval or a large cumulative moment magnitude on an interval does not necessarily mean a high seismic release of energy.
- When working with a shorter catalogue, small changes have a big influence.
- Depending on the processed catalogue, 3 or 4 intervals of high energy release can be observed. By working with a shorter catalogue, "hidden" intervals can be highlighted.
- The intervals of 90-110 km, 120-135 km, 145-150 km with high percentages of released energy resulted from the analysis are in accordance with the weaker rupture plans proposed by Ganas et al. (2010) through the theory of stress transfer and with the unstable triple junction model proposed by Beşuţiu (2006).
- The 95-105 km range proposed in various works as an aseismic interval has a low percentage of energy release only if the 1940-2019 catalogue is considered; otherwise this interval is included in the high energy release area of 90-110 km.
- The 110-120 km aseismic range proposed by Bălă et al. (2019) can be seen in all the catalogues.
- The "hidden" interval highlighted by the 1940-2019 catalogue (75-85 km) is according to Oncescu (1984) in the low speed zone, having the capacity to generate a maximum earthquake of Mw = 7 (Pavel et al. 2015).
- The interval of 90-110 km has the capacity to generate a maximum earthquake of Mw = 8, and the segments 120-135 km and 145-150 km of Mw = 8.1 (Pavel et al. 2015).
- Above 75 km depth and below 150 km depth the energy release is very small, in close agreement
  with the observations made by Radulian et al. (2018), but one should consider that for the
  historical earthquakes in the ROMPLUS catalogue the depths of the ruptures may have small
  variations.

In order to estimate more restricted latitude and longitudinal coordinates, the ROMPLUS catalogue 984-2019 was computed The analysis was made calculating the cumulative energy on rectangles of 0.2°N x 0.4°E and depth intervals of 10 km starting from a depth of 60 km, keeping on each depth range the horizontal area where the cumulative energy exceeded 90% of the total energy over the respective depth range (Figures 20 and 21). The results are in agreement with the energy dissipation centres proposed by Beşuţiu et al. (2009) and tend to support the model of triple unstable junctions.

.

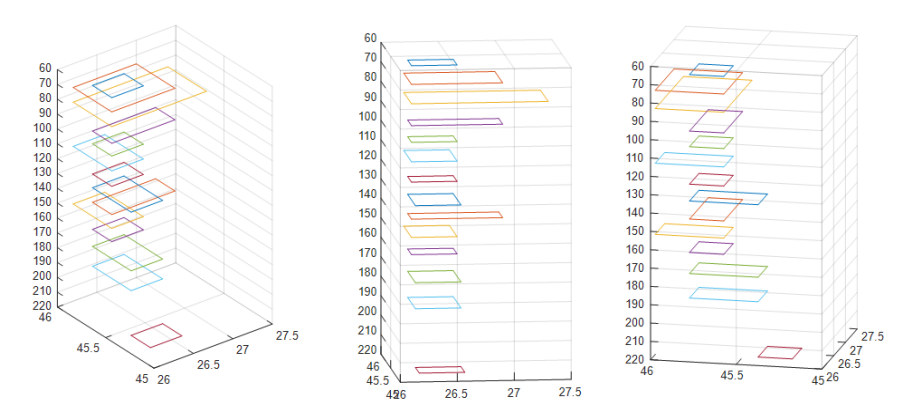


Figure 20. 3D distribution of the surfaces containing the hypocenters in which the cumulative released energy of the earthquakes exceeded 90% of the total energy released over the respective depth range

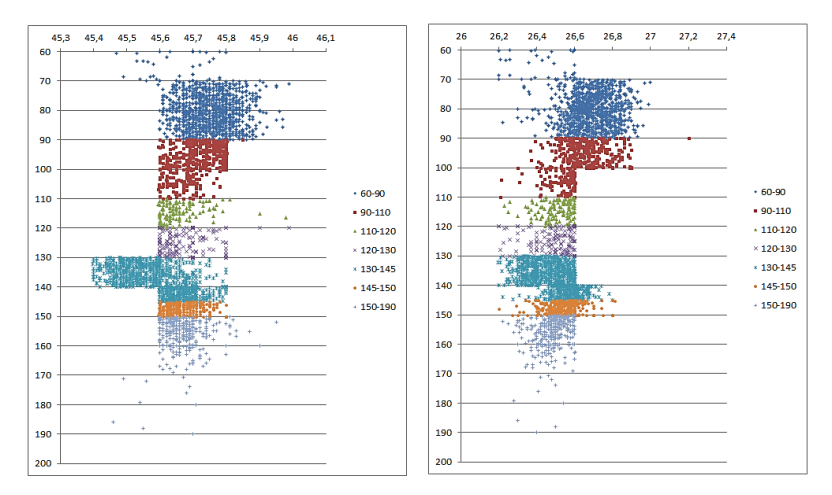


Figure 21. Depth distribution of hypocenters according to latitude and longitude in the area where the cumulative energy exceeded 90% of the total energy released over the respective depth range

In reality, the source of an earthquake is not a point, but a surface. The stochastic simulation is performed either by simplifying the source by considering it a point (SMSIM - its geometry being taken into account through the effective distance, if desired), or by considering the source as a finite fault (EXSIM). At the same time, the estimation of the hypocenters cannot be restricted to the point level because the generation of an earthquake is random and the potential rupture surfaces may change at each seismic event. In this section the seismic centres (in volume coordinates) that historically have the greatest energy release were identified.

#### 4.3. Path duration

In stochastic simulations, the path duration is given by a distance function defined at intervals and it includes both the influence of the mediums from the source to the bedrock and the influence of local site conditions. Boore and Thomson (2014) determine the function of the S-wave path-dependent duration for the NGA-West2 database of 15,923 records. They determine the significant duration in which 5% to 95% of the seismic energy is released (D<sub>95</sub>) for each record. From this duration they eliminate the source duration and observe a quite random distribution of the average duration with distance. The randomness is given by the fact that in some cases the threshold of 5% of total energy is reached too early due to the influence of P waves, and in other cases the 95%

threshold is reached too late due to local site conditions effects. In order to avoid these influences, they propose the following formula for calculating the significant duration:

$$D'_{95} = 2(D_{80} - D_{20}) (30)$$

where  $D_{20}$  is the time at which the released seismic energy reaches the percentage of 20% (percentage chosen to avoid the influence of P waves), and D80 the time at which the released seismic energy reaches the percentage of 80% (a value chosen subjectively depending on the match of the window function used in simulations).

The same algorithm was used in the doctoral research with which, based on several hypotheses, the distance dependent path duration was determined. The used database was the same as the one from which the shaping window function was determined (Chapter 2 - 169 accelerograms recorded during earthquakes from 04.03.1977, 30.08.1986, 30.05.1990, 31.05.1990 and 27.10.2004). Source duration was calculated based on the source frequency determined according to Gusev et al. (2002). For the calculation of the path duration, the following hypotheses were analysed for two databases (Database 1 - the 169 horizontal components used to determine the window function and Database 2 - 162 horizontal components used to determine the window function without the records from the Focsani Basin perimeter):

- a) the path duration is determined as the significant duration in which 5% to 95% of the seismic energy is released ( $D_{95}$ ) from which the source duration is eliminated;
- b) the path duration is determined as double the significant duration in which 20% to 80 of the seismic energy is released (D'<sub>95</sub>) from which the source duration is eliminated (Boore and Thompson, 2014).

As can be seen from figure 22, in the range of 90-150 km source to site distances the source duration has a greater influence than the path duration. As can be seen from the differences between the averages for the two databases, the topographic effects of the Focsani Basin strongly influence the path duration. Greater durations compared to other accelerograms from the same source to site distance range were observed also at the seismic stations from Bacau, Adjud, Roman and Bârlad, cities situated in valleys.

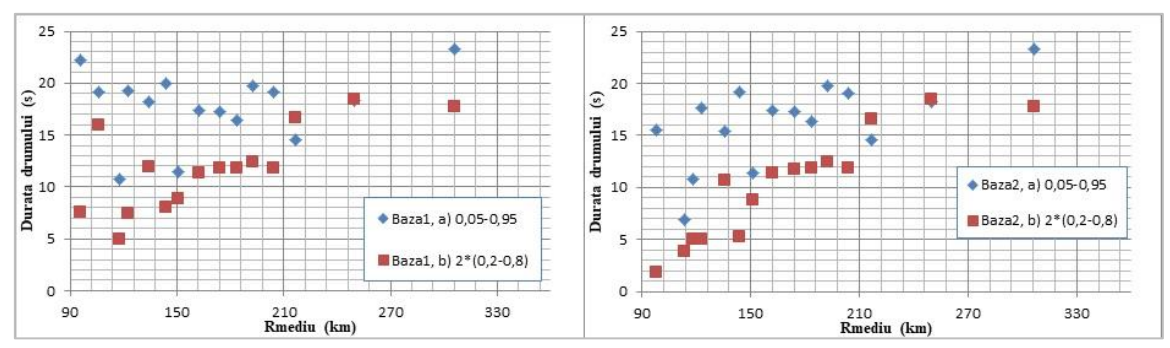


Figure 22. Average values of path durations reported to source - site distances ranges for Database 1 (169 horizontal components of the ground motions recorded during the 04.03.1977, 30.08.1986, 30.05.1990, 31.05.1990 and 27.10.2004 earthquakes), and for Database 2 (records from Database 1 without the ones from Focsani Basin). The intervals on which the average durations were calculated were from 10 to 10 km until 210 km, then the durations were averaged over the 210-230 km, 230 -250 km and 270-350 km ranges due to the fewer data recorded in this intervals

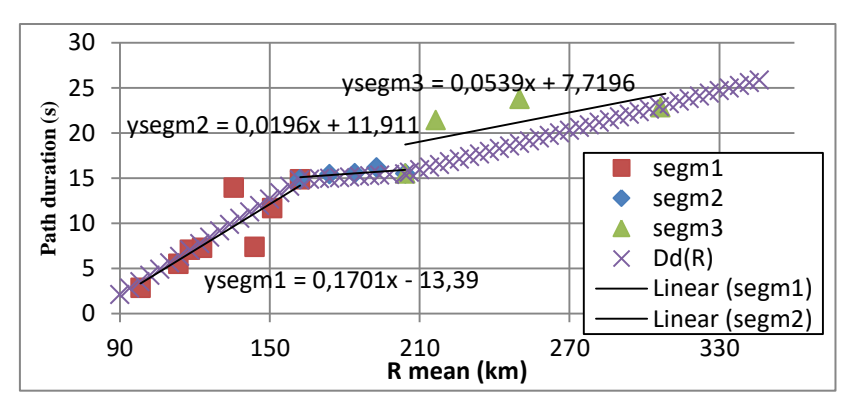


Figure 23. The average values of the path durations for Database 2 divided in three interval segments, with theirs regression lines and the proposed path dependent duration model Dd(R) given in table 11

Table 11. The proposed path dependent duration model

Path duration model							
R (km) Dd (s)							
78	0						
162 11.56							
204	12.30						
Last slope 0.055							
$Dd(R)=Dd(R_{last})+s$	slope * $(R - R_{last})$						

In the stochastic simulation programs the path duration is defined through segments. Based on the b hypothesis for the database 2 from which the records from the Focsani Basin were eliminated, a path dependent duration model was defined (Table 11). In the 205-350 km source to site range there were few recordings, therefore the last segment of the model should be used with restraint, and for this segment another research with another type of determination method should be done (eg. simulations using the finite element method for calculating the path duration). The path duration is dependent on the magnitude, and the database contains ground motion records from all the Vrancea earthquakes with magnitude at least 6. Also, the combination of the database with accelerograms from other intermediate-depth seismic sources similar to Vrancea will not lead to a realistic result because the path duration depends on the local geology.

#### 4.4. Conclusions

The ground motion stochastic simulation methods comprise the characteristics of the source, the path and the changes given by the local site conditions. Numerical simulation methods can also be used to quantify the effects of local site conditions. Whether one chooses a purely stochastic method or a hybrid method, the success of the method depends on establishing the characteristic parameters. Determining the parameters for the simulation of the ground motion is essential, each parameter influencing the final result, and a poor estimation can lead to a less realistic realization. This chapter aims to search and adopt a set of parameters with which one can simulate hypothetical Vrancian earthquakes. In the diagrams below one can find all the parameters of the source, of the path and the general parameters of the local site conditions necessary to simulate the seismic motion with the SMSIM and EXSIM programs. Regarding the characteristics of the shallow geological package, they must be determined for each location where the simulation is generated.

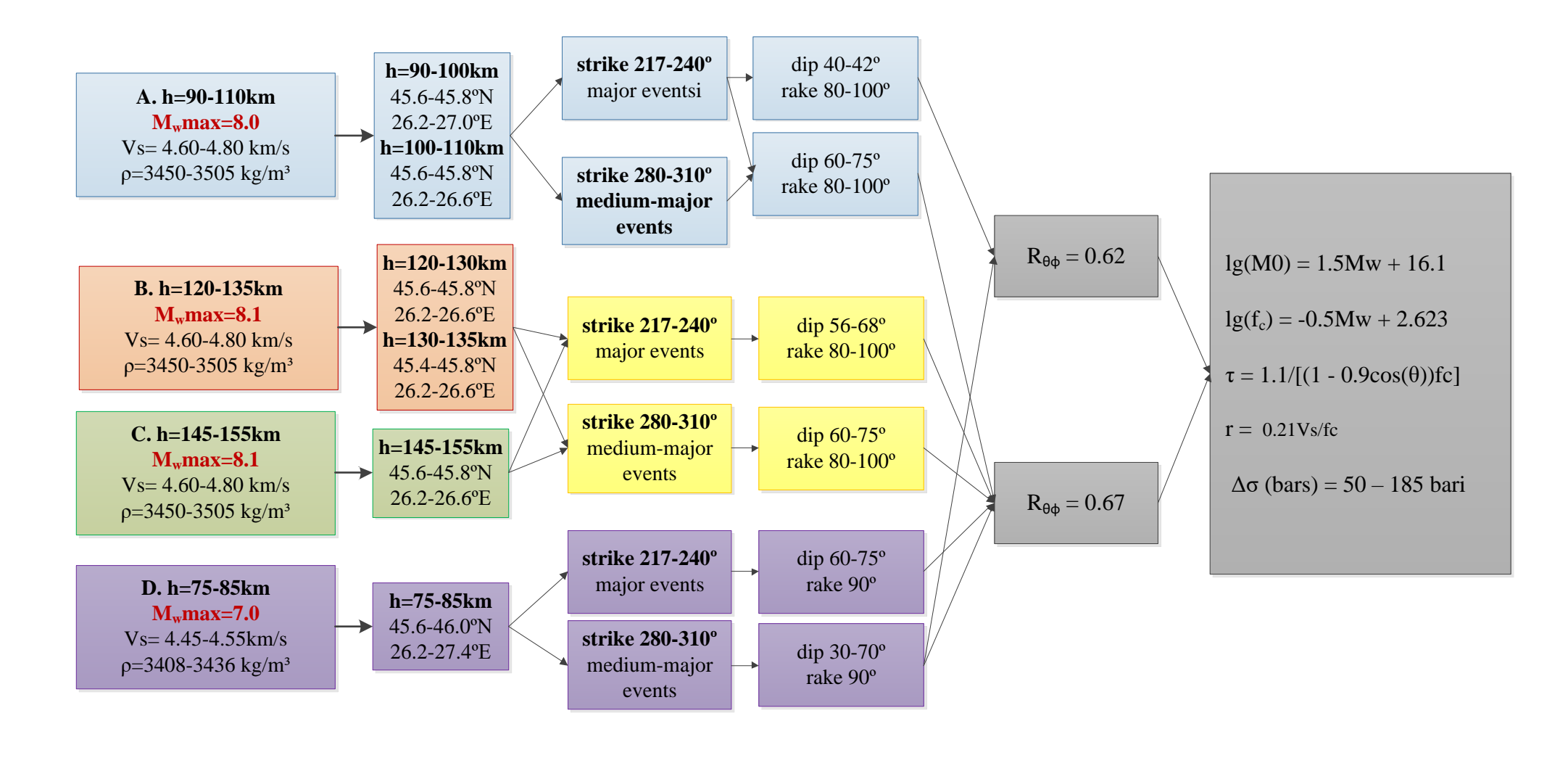


Figure 24. Illustration of the possible source-specific parameters, at depth intervals, necessary for simulation of ground motions generated by Vrancea intermediate-depth seismic source

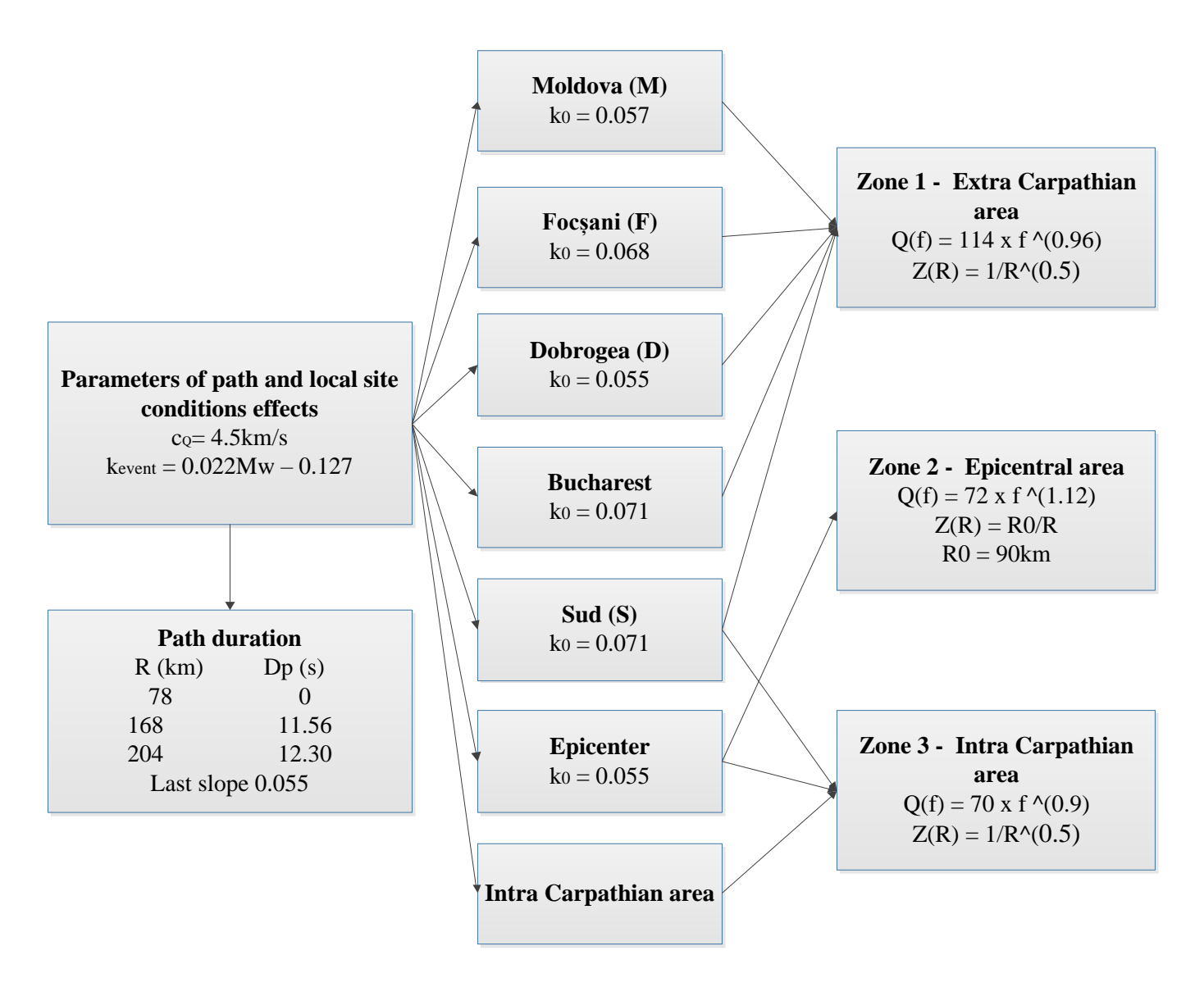


Figure 25. Illustration of the possible path-specific parameters necessary for simulation of ground motions generated by Vrancea intermediate-depth seismic source

# 5. Simulation of accelerograms specific to Vrancea intermediate-depth major seismic events

### 5.1. Introduction

Successful simulations are dependent on how the phenomena are defined, on the parameters that describe them, on taking into account the specificities of each seismic source and the geological package traversed by the waves. The input data should be obtained after a thorough research and the general methods should be adapted to particular cases. The previous chapters have detailed how the method was modified to best describe the specific behaviour of the ground motions generated by the Vrancea intermediate-depth source. Also, a detailed study of all the parameters included in the simulation calculation was presented in the thesis, and where there were no specific studies in the literature, the phenomena and parameters were defined. Intuitively, the next step to be taken in using the proposed method is a test and validation step.

Thus, to verify the accelerogram simulation method, simulations were performed for the INCERC site (Bucharest) for the ground motions produced by the earthquakes of August 30, 1986 Mw = 7.1) and March 4, 1977 (Mw = 7.4). Being earthquakes with large magnitudes, it is expected that the surface geological layers will have nonlinear behavior, which means that the stochastic method implemented in SMSIM will not be able to fully capture the wave modification phenomena. In order to correctly simulate the contributions of all the parameters, SMSIM will be used to simulate the seismic motion at the bedrock level, then the DEEPSOIL program will be used to take into account the changes produced by the behaviour of local site conditions. Combining the two programs the simulation method becomes a hybrid method composed of a stochastic and a deterministic method.

Due to the fact that for certain parameters in the literature there are several variants, the verification had several intermediate steps in order to establish them. Thus, for the attenuation given by the wave path, a set of simulations was performed for each of the 6 proposed attenuation functions (Oncescu, et al., 1999; Radulian, et al., 2000; Oth, et al., 2008; Pavel, 2015; Pavel & Vacareanu, 2015; Pavel & Vacareanu, 2018), the function that best estimates the attenuation being that proposed by Oth et al. (2008). As a definition of local site conditions there are 3 geological profiles of different depths for the INCERC site: Constantinescu and Enescu (1985) with a profile of approximately 1100m, Lungu et al. (1998) with a profile of 127m and Neagu (2015) with a profile of 153m (this profile is actually the location of the seismic station in CNRRS-INCERC, not the exact location of the registered accelerograms). The definition of local site conditions raised several problems that were discussed in the thesis: the problem of discretization, the problem of the stratification depth considered in the calculation and the problem of the stratification model considered. Another parameter that proved to be problematic due to the high sensitivity of the results in relation to it was the corner frequency of the source spectrum.

In order to perform the simulations at the bedrock, the code of the SMSIM set of programs has been modified to take into account the particularities of the Vrancea-intermediate source.

## 5.2. Simulation of the INCERC site accelerograms generated by the Vrancea intermediate-depth earthquake of August 30, 1986

For the accelerogram simulation specific to the earthquake of August 30, 1986, an equivalent linear and nonlinear analysis was performed with DEEPSOIL for a set of 20 simulations performed with the modified SMSIM. As it can be seen from Figure 26, both nonlinear and equivalent linear analysis approximate well the spectral amplitude peaks; the equivalent linear one having slightly higher amplitudes for certain periods. However, with respect to the peak values of the ground accelerations, it can be seen from table 12 that the nonlinear analysis decreases, on average, the motion by approximately 20 20 cm/s<sup>2</sup>, while the linear equivalent analysis estimates well the PGAs. The difference between the two analyses that quantify the contribution of the superficial soil stratification does not show that the soil did not have a nonlinear behaviour, but that the nonlinear analyses of the soil's behaviour and the way in which it modifies the seismic wave are a field under research for the specific conditions from Bucharest; equivalent linear analysis is a simplified analysis better covered by research, and this type of analysis is also recommended as a non-linear analysis verification.

Figure 26 shows that the nonlinear analysis "spreads" the energy from the first abrupt energy release segment to the second segment, and this transforms the initially pulse-like accelerogram into an accelerogram with gradually decreasing amplitude peaks. The equivalent linear analysis instead, retains the first segment of sudden energy release (acceleration pulse containing on average 50% of energy). Regarding the significant duration (the period in which 90% of energy is released, from the moment of exceeding the first 5% to reaching the 95% percentage), both analyses extend the significant duration on average by approximately 2s for the equivalent linear analysis and 7s for nonlinear analysis. For the equivalent linear analysis the difference can be explained by the influence of the P waves from the real seismic motion (SMSIM is a program to simulate the S waves, the energy of the P waves not being taken into account). The larger difference of the significant duration resulted from the nonlinear analysis is given by the change in the energy distribution explained above.

To choose the most suitable simulation, a misfit analysis was performed based on Karimzadeh's (2019) article for the following parameters: peak acceleration PGA, peak velocity PGV, ratio between peak acceleration and peak velocity PGV/PGA, cumulative absolute velocity CAV, Arias intensity Ia, significant duration t<sub>eff</sub> or t<sub>D</sub>, accelerations spectral intensity ASI (performed between 0.1 s and 2.5 s) and pseudo-spectral response acceleration PSA. Figure 26 shows the average misfits for both sets of 20 simulated accelerograms. Although both analyses have very good matching coefficients, it is observed that the equivalent linear analysis generates better simulations.

Table 12. Characteristics of the simulated accelerograms considering a nonlinear and an equivalent linear analysis for modeling the local site conditions

alent iniear anarysis	101 11100011	ing the io	ear site come	
	PGA bedrock	PGA nonlinear	PGA equivalen	
Cimulation	(cm/s <sup>2</sup> )	(cm/s <sup>2</sup> )	linear (cm/s <sup>2</sup> )	
Simulation	(cm/s)			
86INCNS	-	96.9	96.9	
86INCEW	-	109.1	109.1	
Mean - real	-	103.0	103.0	
S1 190	79.2	88.5	117.4	
S1 191	85.3	94.6	112.8	
S1 192	82.8	81.5	92.9	
S1 193	86.0	82.5	112.3	
S1 194	84.2	79.3	92.1	
S1 195	91.0	88.2	108.1	
S1 196	82.5	86.2	101.8	
S1 197	73.2	83.5	92.6	
S1 198	82.9	86.7	109.8	
S1 199	90.0	89.9	111.3	
S1 200	83.5	79.9	116.2	
S1 201	110.6	100.7	163.1	
S1 202	88.1	81.3	101.6	
S1 203	90.8	83.8	90.9	
S1 204	86.1	79.8	88.3	
S1 205	104.1	88.8	90.8	
S1 206	70.8	76.1	92.3	
S1 207	83.0	82.9	107.7	
S1 208	75.6	88.4	94.6	
S1 209	111.2	88.7	143.7	
Mean - simulations	87.0	85.6	107.0	

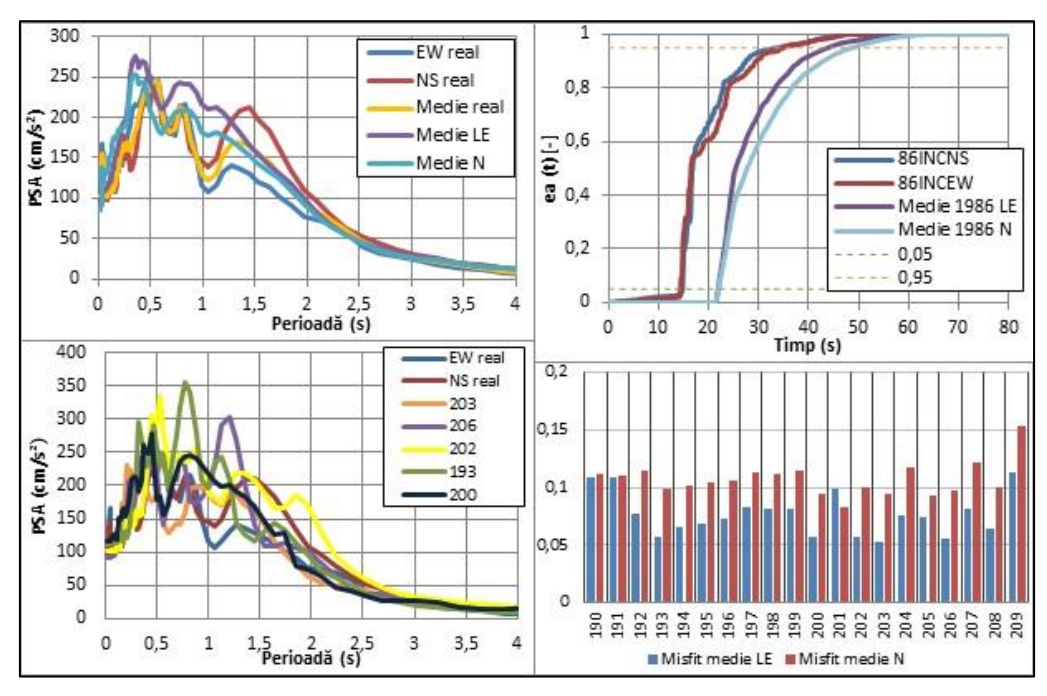


Figure 26. Comparison between the accelerograms recorded at the INCERC station during the earthquake of August 30, 1986 and the simulations performed with the modified SMSIM and DEEPSOIL considering a nonlinear analysis (N) and an equivalent linear analysis (LE) regarding a. the average spectra, b. the normalized cumulative energy c. the spectra of the simulations with the best misfits, d. misfits for all the realizations

# 5.3. Simulation of the INCERC site accelerograms generated by the Vrancea intermediate-depth earthquake of March 4, 1977

For the accelerogram simulation specific to the earthquake of March 4, 1977, an equivalent linear was performed with DEEPSOIL for a set of 20 simulations performed with the modified SMSIM. In figure 27 it can be observed that the average spectra of the 20 simulations falls between the spectra of the two orthogonal recordings NS and EW, approximating very well the average spectra of the two orthogonal directions. Regarding the amplitude parameters (PGAs) it can be seen from table 13 that the average of the simulations is approximately equal to the average of the recordings. The root mean square accelerations and the significant duration are approximately equal to the averages of the real parameters. It is important to note that, as can be seen from figure 27, no simulation significantly exceeds the spectrum of the seismic motion recorded in the NS direction. Also, it is observed that, on average, the peak accelerations from the surface of the site decrease by approximately 90 cm/s<sup>2</sup> from those at the level of the bedrock, which means that the non-linear transformations of the soil occur with the release of a quite high quantity of energy (table 13).

In order to choose the most suitable simulations, three misfit analyses were performed (based on the parameters presented in the previous subchapter): in relation to the average of the two directions and in relation to each orthogonal component in part because the differences between the two records are significant. It can be seen from figure 28 that, compared to the average, all the misfits are less than 0.15, which indicates a very good match with the reality. Regarding to each horizontal component in part, the larger misfits from one direction are counterbalanced by very good misfits in the other direction. The simulations with the best misfits compared to the average are 201, 202, 197, 205 and 196 (having values between 0.052 and 0.064), compared to the EW direction the most suitable simulation is 196 (with a misfit of 0.053), and compared to NS the most appropriate simulation is 209 (with a misfit of 0.085). In figure 29 and in table 13 are the amplitude, spectral and duration characteristics for the simulations that best reproduce the characteristics of the real ground motions from the INCERC (Bucharest) site recorded during the Vrancea intermediate-depth March 4, 1977 earthquake.

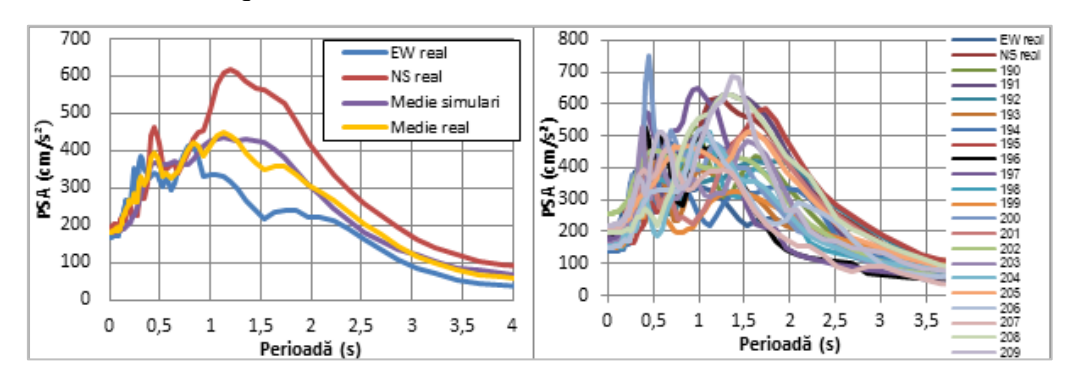


Figure 27. Comparison between response spectra of simulations and those of the INCERC ground motion recordings of the March 4, 1977 seismic event

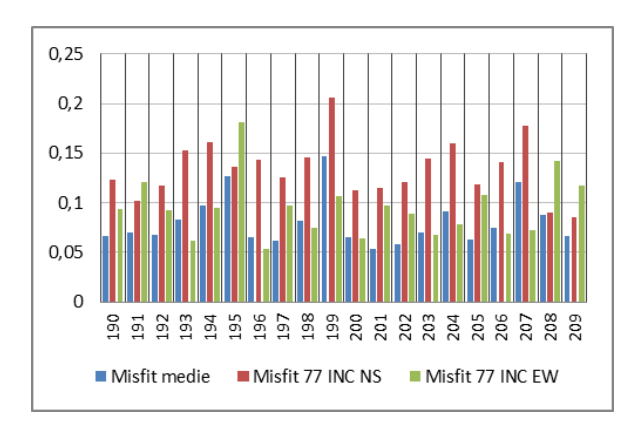


Figure 28. Average misfits between the simulations and the recordings (blue - in relation to the average of the two directions, red - in relation to the NS component, green - in relation to the EW component)

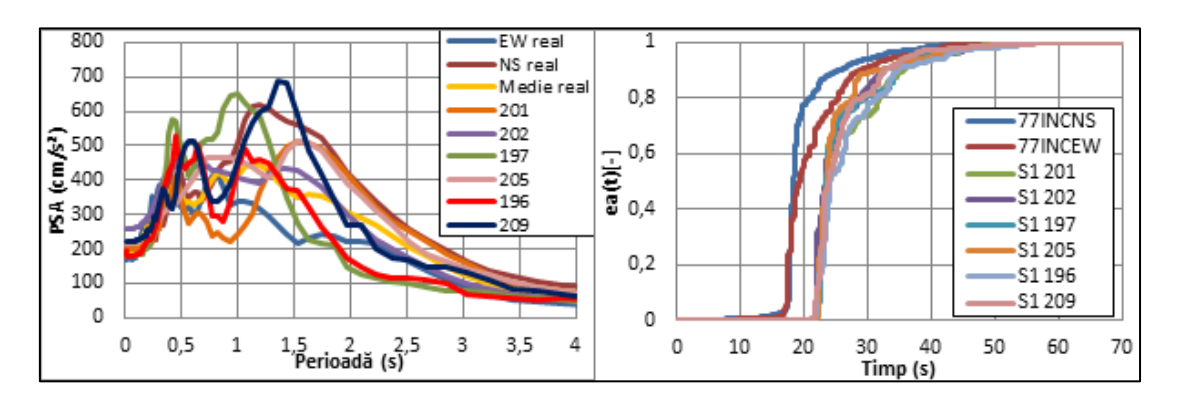


Figure 29. Characteristics of the simulations with best misfits

Table 13. Characteristics of the simulated accelerograms considering an equivalent linear analysis for modeling the local site conditions

	PGA bedrock	PGA surface	Root mean square	Significant
Simulation	$(cm/s^2)$	$(cm/s^2)$		duration (s)
77INCNS	-	193	55	14.14
77INCEW	-	165	36	18.42
Mean - real	-	179	45	16.28
S1 190	332	172	45	14.78
S1 191	282	179	55	13.64
S1 192	284	198	44	15.47
S1 193	250	162	39	18.86
S1 194	270	138	42	16.58
S1 195	281	163	58	11.66
S1 196	244	176	39	20.53
S1 197	309	177	45	16.75
S1 198	254	149	40	19.30
S1 199	217	147	30	21.25
S1 200	264	203	45	18.97
S1 201	240	198	44	17.49
S1 202	294	256	45	16.78
S1 203	226	161	43	15.98
S1 204	221	156	38	19.43
S1 205	329	214	43	17.96
S1 206	255	150	43	17.42
S1 207	264	206	33	19.61
S1 208	332	195	54	14.00
S1 209	317	220	57	14.85
Mean - simulations	273	181	44	17.07

# 5.4. Simulation of the INCERC site accelerograms generated by some Vrancea intermediate-depth scenario earthquakes

The utility of the simulated accelerograms is given by the possibility to reproduce the ground motions in locations where there are no recordings, for quantifying the historical earthquakes and for predicting the level of the seismic hazard for various possible scenarios. The simulation of the recorded motions is only useful for verifying the chosen simulation methods and the definitions of the phenomena that generate and modify the seismic waves. For this purpose, eight earthquake scenarios specific to the Vrancea intermediate-depth source were defined and simulations were performed at the INCERC (Bucharest) site using the hybrid method defined when generating the accelerograms of August 30, 1986 and March 4, 1977 earthquakes.

Based on the parameters presented in Chapter 4, four earthquake scenarios specific to hazard analyses (A, B, C, D - table 14) and four scenarios specific to the design requirements (the limit states and the importance-exposure classes according to P100-1/2013) (table 15) were defined. When verifying the method by simulating the motions generated by the events of 1977 and 1986, it was observed that the corner frequency of the source spectra significantly changes the simulations even if the parameter is chosen from the range of the confidence interval. As a first step an evaluation was performed for counting the spectra's corner frequency influence. Thus for the A scenario 3 variants of 20 simulations were performed: in the first variant the corner frequency was defined according to Gusev et al. (2002), in the second one was defined according to Frankel et al (1996), and in third variant it was used the formula with whom the simulations of the ground motions generated by the 1977 event were made (for this event Gusev et al. (2002) gave the value of the corner frequency with its confidence interval; in order to obtain an appropriate value from the given interval the general relation from Gusev et al. (2002) needed to be slightly changed).

The differences between the corner frequencies of these variants are of the order of the accepted errors, but these variations greatly influence the simulations. In order to illustrate the most disadvantageous (and most realistic) variant of the scenarios, the results of the scenarios in which the source corner frequency was defined according to the simulations of March 4, 1977 event will be further illustrated (variant 1 and 2 underestimate significantly the motions compared to 1977 recorded motions and it should be mentioned that A scenario is defined with a magnitude of 8.0 and its effective distance is approximately 10 km less than the one from 1977). For all the scenarios, the newly defined two-interval window with the "mean" parameters from the 3.4 Subchapter was used, and for the duration extension parameter the value recommended by Boore (2003) was used.

Table 14. The parameter values considered in the scenarios specific to hazard analyses

	e parameter values co							
Parameters	A scenario	B scenario	C scenario	D scenario				
Mw	8.0	8.1	8.1	7.0				
h (km)	100	130	150	80				
Epicenter	45.7° lat. N	45.6° lat. N	45.7° lat. N	45.8° lat. N				
	26.6° long. E	26.4° long. E	26.4° long. E	26.6° long. E				
Source to site distance- R <sub>eff</sub>	175	188	211	175				
Fault geometry Strike/Dip (°)	220°/70°	218°/62°	225°/63°	236°/63°				
Fault dimensions Length/width (km)	28.84/28.84	32.36/32.36	32.36/32.36	8.82/8.82				
Density near source (g/cm <sup>3</sup> )	3.45	3.45	3.45	3.41				
Velocity near source (km/s)	4.60	4.60	4.60	4.45				
Radiation pattern	0.67	0.67	0.67	0.67				
Source spectra	1	1	1	1				
1	$S = \frac{1}{(1 + \frac{f}{f_c})^2}$	$S = \frac{1}{(1 + \frac{f}{f_c})^2}$	$S = \frac{1}{(1 + \frac{f}{f_c})^2}$	$S = \frac{1}{(1 + \frac{f}{f_c})^2}$				
Source corner frequency *V1: Gusev et al. (2002) *V2: Frankel et al. (1996) *V3: Subchapter 5.3	V1: 2.48 – 0.5 <i>Mw</i> V2: 2.623 – 0.5 <i>Mw</i> V3: 2.779 – 0.5 <i>Mw</i> V1: 0.02463Hz V2: 0.0419Hz V3: 0.0601Hz	2.779 — 0.5 <i>Mw</i>	2.779 – 0.5 <i>Mw</i>	2.779 — 0.5 <i>Mw</i>				
Geometrical scattering	$R^{-0.5}$	$R^{-0.5}$	$R^{-0.5}$	$R^{-0.5}$				
Source duration including directivity effect	0.1385	0.1805	0.2425	0.2556				
Path duration	78.0 0.0 162.0 11.56 204.0 12.3 0.055							
Event dependent attenuation k <sub>event</sub>		0.022 <i>Mw</i>	y — 0.127					
Path dependent attenuation		114 <i>f</i>	c 0.96					
Local site conditions			tinescu and Enescu (198	85)				
Shaping window ("mean"	$1.005517(\frac{t}{t_e})^{0.000656}\epsilon$							
parameters, case I, Subchapter 3.4)	$ \begin{array}{c} (2003) \\ t_0 = 2.5 \text{ s} \end{array} $	$0.7026(\frac{t}{t_e})^{0.000575}e^{1.864424(\frac{t}{t_e})}$ second interval; $f_{tb}=2$ *recommended value Boore (2003)						
*the transformed parameters were determined using the mean source+path duration of the scenarios								

Table 15. The parameter values considered in the scenarios specific to design requirements

Parameters	SLS Scenario	USL cl. III Scenario	USL cl. II Scenario	USL cl. I Scenario
Mw	7.06	7.38	7.45	7.55
Source to site	164	166	164	162
distance D (km)				

Table 16. Characteristics of accelerograms simulated according to the scenarios specific to hazard analyses

	A scena	rio	B scena	B scenario		C scenario		nario
	PGA	Tc	PGA	Tc (s)	PGA	Tc (s)	PGA	Tc (s)
Simulation	$(cm/s^2)$	(s)	$(cm/s^2)$		$(cm/s^2)$		$(cm/s^2)$	
S1 190	222	2.15	166	1.74	148	1.60	119	1.10
S1 191	211	1.61	220	2.15	196	1.83	149	1.33
S1 192	166	1.63	220	1.74	204	1.68	139	1.21
S1 193	183	1.67	177	2.57	162	1.80	148	1.09
S1 194	228	1.63	160	1.85	210	2.09	177	1.34
S1 195	214	2.00	219	1.49	222	2.37	197	0.79
S1 196	163	1.54	181	1.91	132	2.10	180	1.54
S1 197	224	1.46	163	1.59	181	1.95	172	0.78
S1 198	155	2.00	223	2.21	193	1.52	132	1.04
S1 199	206	2.41	180	1.32	143	1.58	170	0.76
S1 200	199	1.97	212	1.59	166	1.63	190	1.33
S1 201	225	1.74	162	2.23	209	1.66	152	1.27
S1 202	204	1.97	256	2.08	182	2.07	136	1.11
S1 203	227	2.05	183	2.13	163	2.14	157	0.50
S1 204	266	1.80	249	2.03	229	1.98	160	1.29
S1 205	184	1.64	135	1.61	186	2.16	139	1.42
S1 206	200	2.13	174	1.32	172	1.60	175	1.49
S1 207	161	1.14	253	2.23	227	2.12	153	0.81
S1 208	195	1.36	251	2.00	178	1.55	143	1.35
S1 209	178	1.97	193	1.49	213	1.63	127	0.83
Mean	200	1.79	199	1.86	186	2.03	156	1.12

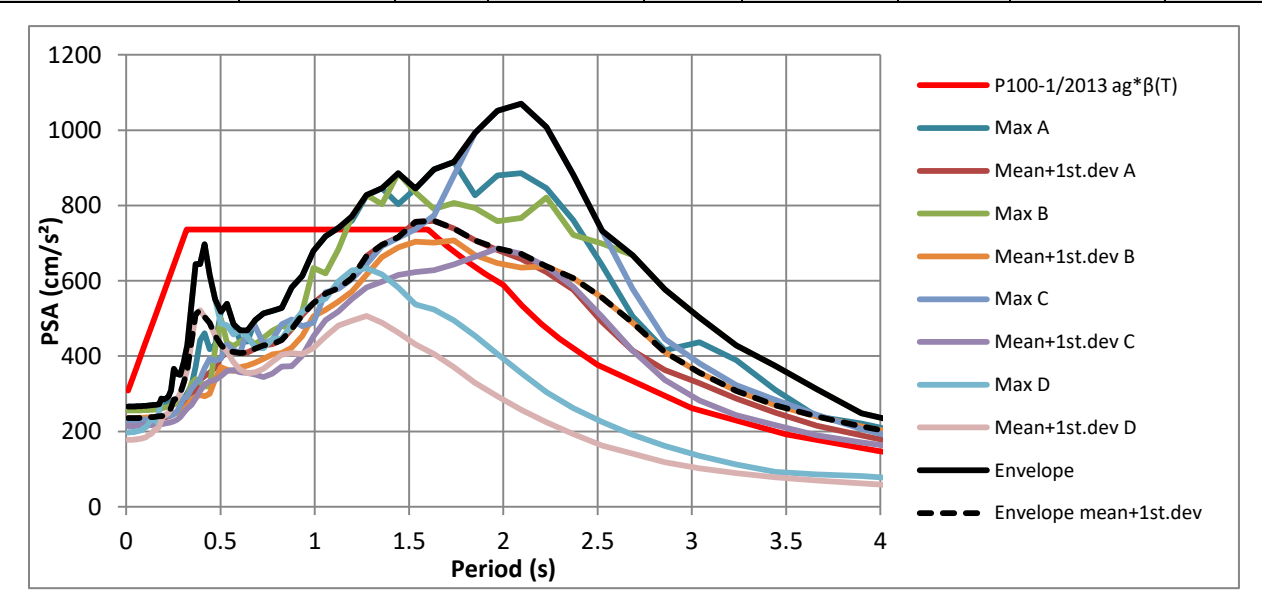


Figure 30. Spectral statistical descriptors for the simulation sets performed for each scenario and the envelope of all four scenarios specific to the hazard analyses

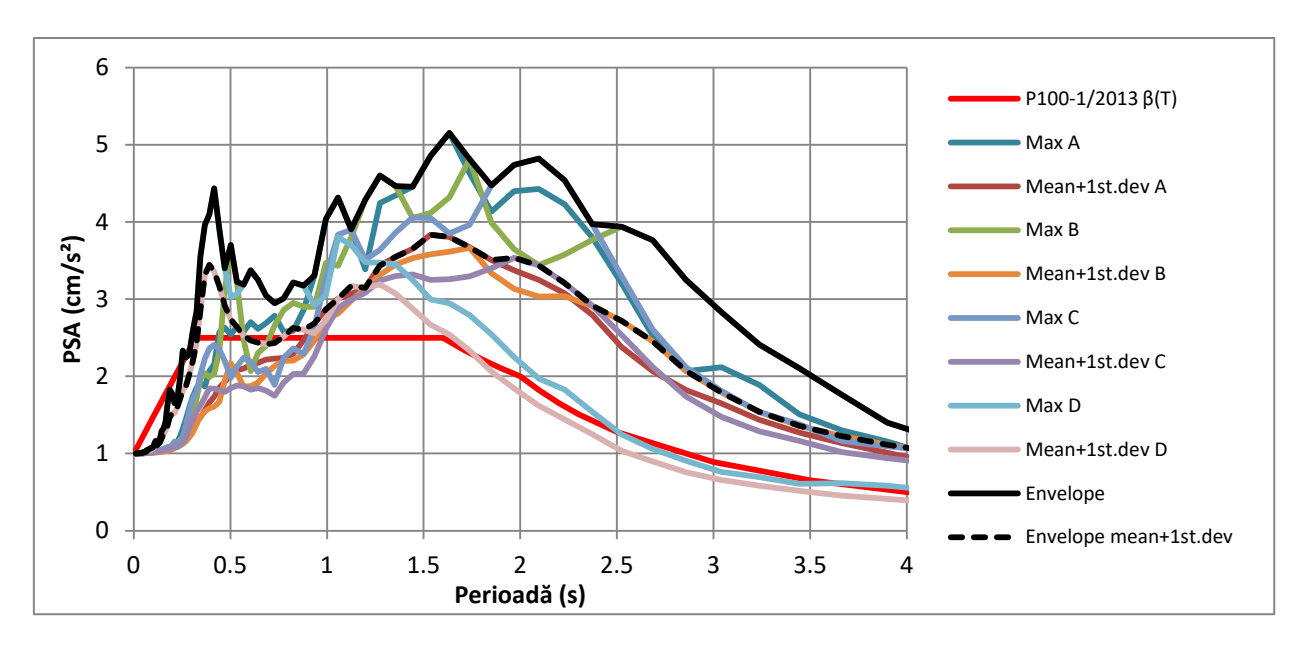


Figure 31. Statistical descriptors of the normalized spectra for the simulation sets performed for each scenario and the envelope of all four scenarios specific to the hazard analyses

As a general aspect, the corner period increases up to 2.57 s, the average corner period of the simulations performed for scenarios A, B and C exceeding the corner period proposed by the design code P100-1/2013 by 0.2-0.4 s. The maximum peak accelerations of the scenarios are 265 cm/s² for scenario A, 255 cm/s² for scenario B, 228 cm/s² for scenario C and 196 cm/s² for scenario D. But it should be noted that the bedrock the peak accelerations decrease until the surface on average by 150-200 cm/s² for scenarios A and B and by 100-50 cm/s² for scenarios C and D, which means that the non-linear transformations of the superficial soil layers occur with very high energy discharge, and for a location with a shallower stratification the ground motions could record much higher peak accelerations. Also, relative to the code, the PGA (ag) dictates the anchoring point of the design spectrum (when the period is 0.01) and it is the amplification value of the normalized spectrum  $\beta(T)$ . Taking into account that the illustrated spectra of the simulations do not result from the same algorithm as the code spectrum, it should be mentioned that the only implication of the smaller PGAs of the simulations is that for small periods (below 0.25s - very rigid structures) there is a difference of up to 100 cm/s² between the spectral accelerations of the simulations and the hazard level proposed in the code.

It is observed that, for the INCERC local site conditions, a major earthquake produces larger spectral amplitudes for periods longer than 1s. The motion from the bedrock loaded with short periods and with high acceleration peaks is transformed by the behaviour of the superficial layers in a motion rich in long periods, with lower acceleration peaks (due to the energy dissipation during the processes of nonlinear deformation of the soil). Another general observation is that the package of soil layers by which the local site conditions have been defined has an own period of about 5.5 s, which means that for earthquakes of greater magnitude, the tendency to increase the corner period may continue.

Regarding the spectral characteristics it is observed that until the period of 1.0 s the simulations of scenarios A, B and C have smaller amplitudes by about 200-300 cm/s<sup>2</sup> compared to the spectrum of the Seismic Design Code P100-1/2013, but the smaller scenario (D) produces larger amplifications for periods smaller than 1.0 s. The design spectrum from the code was defined using

accelerograms recorded during the earthquakes of March 4, 1977 (Mw = 7.4), August 30, 1986 (Mw = 7.1) and May 30, 1990 (Mw = 6.9). As can be seen from the previous chapter, the 1986 earthquake did not have as much power as that of 1977. The 1986 event did not have enough energy to produce the same level of modification in the soil superficial layers that could lead to many long periods spectral components, so its energy (as in the case of scenario D) remained on the smaller periods spectral components. If it is desired to construct a design spectrum in which to consider, along the real registered motions, simulations performed based on certain scenarios, the magnitude range of the scenarios must be rich to take into account the all the cases (to include different stages of spectral content transformations according to different stages of nonlinear soil behaviour due to the level of introduced stress). It is important to mention that according to Eurocode 8 (SR-EN1998-1:2004, 2004) the soil in the INCERC site (Bucharest) is classified in type C, and the results of the simulations for other types of local conditions will be different.

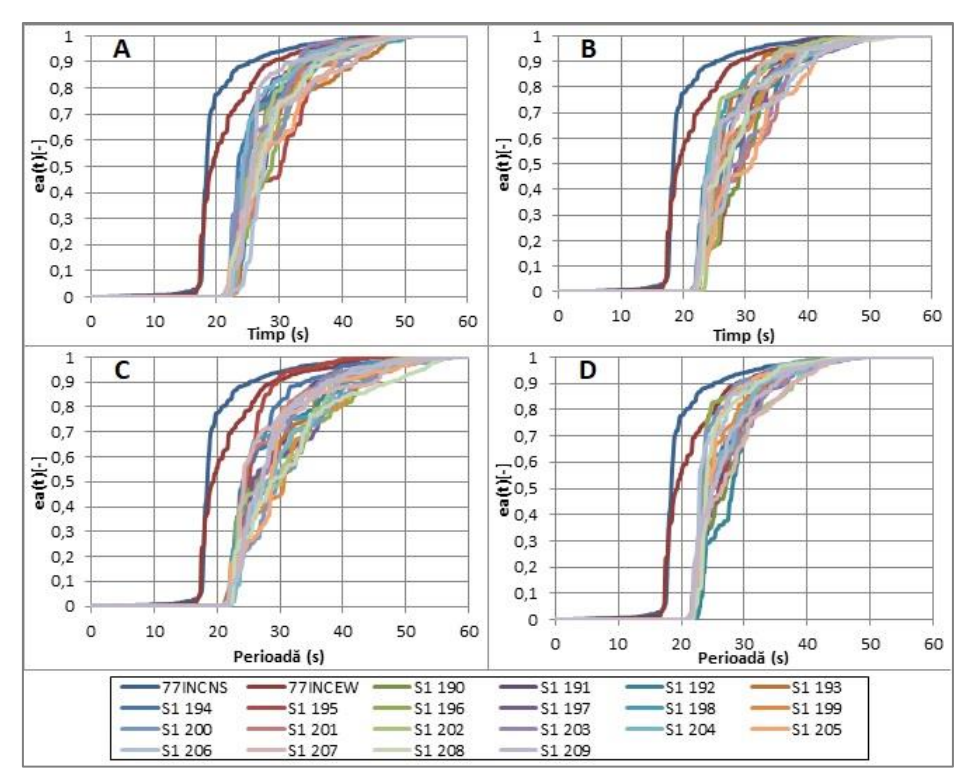


Figure 32. Comparison between the normalized cumulative energies of the accelerograms recorded at the INCERC station during the earthquake of March 4, 1977 and the normalized cumulative energies of the simulations performed for each hazard analysis type scenario

Regarding the normalized cumulative energies, one can observe the "spreading" of energy from the abrupt release segment to the slow release segment of the energy, noting several sequences of strong phase - slow phase (the near vertical segments representing pulse type accelerations with large values, and the inclined segments represent accelerations with lower peak values). This phenomenon indicating the energy losses resulting from the nonlinear changes suffered by the site soil. This "scattering" leads (together with the increase of the source duration produced by the magnitude of the earthquake and the duration of the path) to an increase of the significant duration of up to 10 s comparing to the average of the records of 1977 from the INCERC site (the largest increases being registered for scenario C). Regarding the root mean square accelerations, scenarios A and B have average values of approximately 60 cm/s<sup>2</sup>, indicating an intensity 33% higher than

the average intensity of the accelerograms recorded in 1977. The average values of scenarios C and D fall between the values of the two orthogonal components of 1977.

Considering that the seismic action loads the structures according to their own vibration modes it should be emphasized that from the first three hazard analyses specific scenarios resulted spectral accelerations of up to  $900 - 1100 \text{ cm/s}^2$  for periods greater than 1 s, exceeding the hazard level proposed by the design code with up to  $500 \text{ cm/s}^2$ , which means that in case of a large seismic event, the flexible structures will be loaded with a very high seismic energy.

In the Design Code P100-1/2013 Part I, Annex D. Procedure for nonlinear static calculation of structures (biographical), and Part II, Chapter C3. The seismic action states that "for dynamic calculation of structures accelerograms are used, they can be of several types: artificial, recorded and simulated" " (MDRAP, 2014). Due to the complexity of the simulation methods and the parameters that describe the phenomena that generate and influence the seismic waves, at present there are no simulated accelerograms specific to the seismic hazard in Romania within the reach of the engineers. Considering the fact that the resistance structures of the buildings are designed based on the concept of limit states and classes of importance, the second set of scenarios was realized using the data from the article of Pavel et al (2017) (resulted from the disaggregation of the seismic hazard for the limit states and the importance classes defined in P100-1/2013). Thus, four scenarios are considered for: SLS service limit state for all buildings, ULS ultimate limit state for buildings in the importance-exposure category II, ULS ultimate limit state for buildings in the importance-exposure category II and ULS ultimate limit state for buildings from the category of importance-exposure I. For each scenario, a set of 10 accelerograms was generated based on the defined hybrid method. The 40 resulting simulations are attached to the thesis in electronic format.

For the four scenarios realized in the design hypotheses, all parameters except the moment magnitude and the source-site distance were identical. It is observed that the large magnitudes transform the spectral amplitudes corresponding to the short periods into components corresponding to the long periods (Figures 34 and 35). The corner period of the simulated motions increases from the average of 1.51 s for the SLS scenario for all buildings to the average of 1.66 for the USL scenario for buildings of the importance-exposure category I. It is also observed that the mean root square accelerations increase with increasing magnitudes from an average of 42.77 cm/s² (SLS scenario for all buildings) to 57.84 cm/s² (USL scenario for buildings of importance-exposure category I). Regarding peak accelerations, there is an increase of the differences between the accelerations at the bedrock level and those at the level of the free surface as the size of the hazard increases (for SLS for all buildings the peak acceleration from the surface is 50 cm/s² lower than the one from the bedrock level while for USL for buildings in the importance-exposure category I is 115 cm/s² smaller). This increase in differences once again demonstrates an increase in the amount of energy dissipated due to the nonlinear behaviour of the superficial soil layers in the INCERC site (Bucharest).

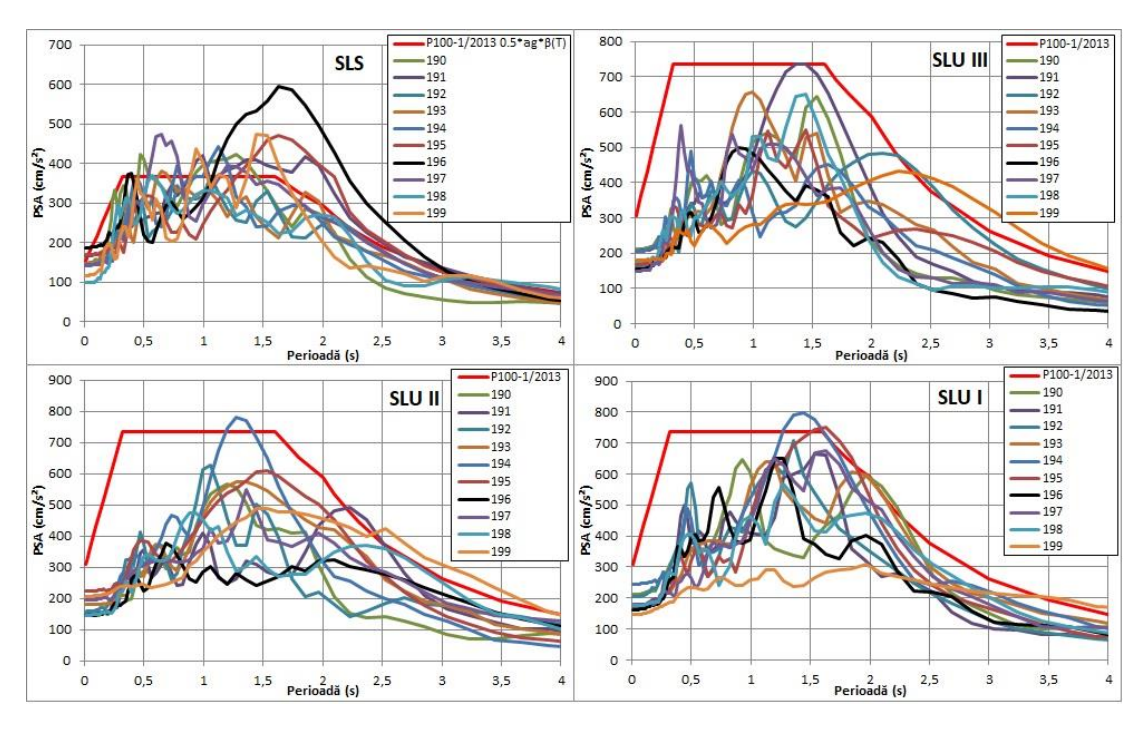


Figure 33. Comparison between the spectra of the recorded accelerograms at the INCERC station during the earthquake of March 4, 1977, the elastic response spectrum from P100-1/2013 and the spectra of the simulations performed for the SLS, USL class III, USL class II and USL class I scenarios

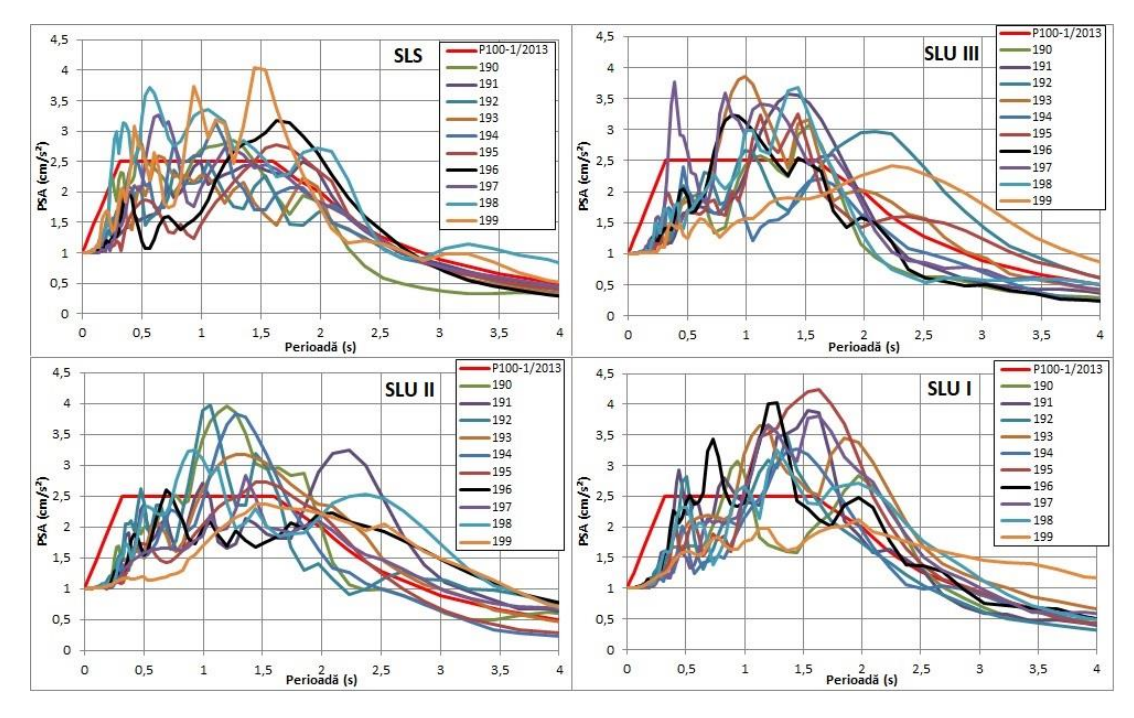


Figure 34. Comparison between the normalized spectra of the recorded accelerograms at the INCERC station during the earthquake of March 4, 1977, the normalized elastic response spectrum from P100-1/2013 and the normalized spectra of the simulations performed for the SLS, USL class II, USL class II and USL class I scenarios

Table 17. Characteristics of accelerograms simulated according to the design hypothesis scenarios

	SLS scen	ario	ULS Class III	scenario	ULS Class II scenario		ULS Class l	I scenario
	PGA	Tc (s)	PGA	Tc (s)	PGA	Tc (s)	PGA	Tc (s)
Simulation	$(cm/s^2)$		$(cm/s^2)$		$(cm/s^2)$		$(cm/s^2)$	
S1 190	148	1.29	210	1.54	144	1.34	210	1.82
S1 191	167	1.85	207	1.47	151	2.23	171	1.62
S1 192	146	1.50	163	2.20	157	1.16	203	1.36
S1 193	146	1.60	171	1.26	180	1.54	176	1.83
S1 194	142	1.22	204	1.54	204	1.34	244	1.49
S1 195	169	1.70	168	1.44	222	1.62	177	1.64
S1 196	187	1.72	155	1.18	145	1.86	162	1.27
S1 197	145	1.20	149	1.19	194	1.46	177	1.63
S1 198	100	1.50	177	1.44	146	1.91	175	1.69
S1 199	117	1.52	180	2.40	207	2.19	146	2.29
Mean	147	1.51	178	1.57	175	1.66	184	1.66

Table 18. Characteristics of accelerograms simulated according SLS and ULS cl. III scenarios

Scenario		SLS scenario				ULS Class	III scenario	
	SA@1.0s	SA@1.0s	SA@1.6s	SA@1.6s	SA@1.0s	SA@1.0s	SA@1.6s	SA@1.6s
Simulation	(cm/s2)	/PGA	(cm/s2)	/PGA	(cm/s2)	/PGA	(cm/s2)	/PGA
S1 190	405	2.73	285	1.93	536	2.55	581	2.77
S1 191	355	2.13	387	2.32	542	2.62	654	3.16
S1 192	366	2.50	277	1.90	428	2.63	395	2.42
S1 193	328	2.25	213	1.46	636	3.72	419	2.45
S1 194	409	2.88	281	1.98	246	1.21	451	2.21
S1 195	279	1.65	471	2.79	481	2.86	334	1.99
S1 196	349	1.87	594	3.18	463	2.99	361	2.33
S1 197	332	2.29	346	2.39	498	3.34	383	2.57
S1 198	334	3.34	224	2.24	531	3.00	480	2.71
S1 199	338	2.89	395	3.37	283	1.57	349	1.94
Mean	343	2.45	463	2.70	463	2.70	463	2.70
Standard								
deviation	33	0.49	98	0.67	98	0.67	98	0.67

Table 19. Characteristics of accelerograms simulated according ULS cl. II and ULS cl. I scenarios

Scenario		ULS Class II scenario				ULS Class	I scenario	
	SA@1.0s	SA@1.0s	SA@1.6s	SA@1.6s	SA@1.0s	SA@1.0s	SA@1.6s	SA@1.6s
Simulation	(cm/s2)	/PGA	(cm/s2)	/PGA	(cm/s2)	/PGA	(cm/s2)	/PGA
S1 190	533	3.70	424	2.95	511	2.43	435	2.07
S1 191	372	2.46	275	1.82	408	2.38	660	3.86
S1 192	627	3.99	394	2.51	520	2.56	486	2.39
S1 193	508	2.82	517	2.87	614	3.49	442	2.51
S1 194	587	2.88	560	2.74	566	2.32	728	2.98
S1 195	485	2.18	591	2.66	538	3.04	750	4.24
S1 196	302	2.08	270	1.86	473	2.92	343	2.12
S1 197	424	2.19	380	1.96	511	2.89	677	3.82
S1 198	416	2.85	270	1.85	437	2.50	414	2.37
S1 199	375	1.81	478	2.31	262	1.79	282	1.93
Mean	463	2.70	416	2.35	484	2.63	522	2.83
Standard								
deviation	98	0.67	114	0.43	93	0.45	159	0.80

### 5.5. Conclusions

In this chapter, the ground motions from the INCERC site (Bucharest) produced by the Vrancea intermediate-depth earthquakes of March 4, 1977 (Mw = 7.4) and August 30, 1986 (Mw = 7.1) and the simulation of accelerograms for hypothetical earthquakes have been successfully generated. The hypothetical events were defined after four scenarios specific to hazard analysis and four scenarios specific to design requirements depending on the limit states and importance classes of the buildings (defined according to P100-1/2013). The proposed hybrid simulation method involves using the modified set of programs SMSIM for generating accelerograms at the bedrock level and adding the influence of local site conditions using the linear-equivalent analysis of soil behaviour implemented in the DEEPSOIL program. In order to define the parameters and phenomena that influence the seismic wave, in this chapter, comparative analysis regarding the wave attenuation function and the way of defining the stratification of the local site conditions were made. Regarding the corner frequency of the source spectrum, significant variations of the simulations were observed when small variations of the parameter were made. Regarding the discretization of the geological stratification used in the DEEPSOIL program, it was observed that depending on it the motions with small periods are perceived or not by the program, in this sense an optimal discretization was defined.

Validating the method by simulating the accelerograms generated by the intermediate-depth earthquakes from March 4, 1977 and August 30, 1986, eight earthquake scenarios for different focal depths and magnitudes were defined and accelerograms were simulated. It was observed that regarding the spectral composition the hazard level proposed by the seismic design code P100-1/2013 is lower for periods greater than 1 s compared to certain simulated accelerograms, with significantly higher spectral amplitudes for the periods up to at 2.75-3.0 s. For scenarios A, B, C, USL class II and USL class I the average corner period of the simulations exceeds the value proposed by the design code, the maximum value of the corner period of the simulations being 2.57 s. The 40 accelerograms simulated based on the design hypotheses (SLS for all buildings, ULS for buildings of importance-exposure category III, ULS for buildings of importance-exposure category III and ULS for buildings of importance-exposure category II are annexed to the present paper in electronic format to provide the design engineers with an alternative method of defining the seismic action.

### 6. Conclusions, personal contributions and future research directions

In this paper, a method of generating the simulated accelerograms is modified and applied. Based on a thorough research, simulations for the Vrancea intermediate-depth source have been successfully performed both for seismic motions generated by past events and for earthquake scenarios. The usefulness of the simulated accelerograms is given both by the possibility of their use in the structures design using dynamic calculation methods, as well as by the possibility of using them together with the a recorded accelerograms in hazard analyses (by simulating unregistered historical events or by simulating possible hypothetical events through which one can cover ranges of magnitude not covered by past events and locations where there is no record of seismic motions).

In order to perform the simulated accelerograms, two stochastic simulation methods (with point source and fault source) and two hybrid methods (in which the two stochastic methods were combined with a physical-based numerical method to simulate the nonlinear effects specific to the site surface geological stratification) were initially tested. In this first stage analyses regarding the stress drop parameter, the definitions of the source spectra, the path duration and the local site conditions influence were made. It was also observed that the white noise shaping window implemented in the programs does not capture the specificity of the seismic motions generated by the Vrancian subcrustal events in terms of the time domain energy release.

Based on these observations, a number of 371 horizontal components of the ground motions recorded at different seismic stations during the earthquakes of March 4, 1977, August 30, 1986, 30 and May 31, 1990, October 27, 2004 were analysed and five types of energy release behaviours were defined. The types of behaviour were divided as follows: A category (typical model for almost half of the records) in which about 50% of the energy is released in the first 1.5-3.0 s of the strong motion, while the rest of the energy is slowly released in 20-40 s and B category with the exceptions of type I, II, III and IV. For the ground motions included in A category, the statistical descriptors were determined for each earthquake separately, and for all five earthquakes together. Then, based on the statistical descriptors, the parameters specific to the noise shaping window implemented in the stochastic simulation programs were determined. Realizing that the window defined for the SMSIM and EXSIM programs does not capture the behaviour pursued, a new shaping window was defined, on the basis of which the specific energy release of the motions produced by the Vrancian intermediate-depth earthquakes was simulated.

In the next stage, a thorough research of all the stochastic simulation's input parameters was carried out. Based on the specialized literature, for each parameter comparative analyses were performed and the best methods of defining and quantifying phenomena were established. For some parameters, specific studies have been carried out to determine them, because either there were no studies for defining the parameters, or their definition intervals were too varied and extended. Thus, restricted intervals of focal depths and epicentres were determined and a relationship was defined for the path duration (this parameter was not studied in other papers in the form needed in simulations). Based on this research, possible spatial intervals for future seismic events have been defined, and for each interval there have been defined intervals characterizing the parameters needed to perform the accelerogram simulations.

Subsequently, simulations for the seismic motions produced by the earthquakes of March 4, 1977 and August 30, 1986 at the INCERC (Bucharest) site were successfully performed, and the hypotheses for defining the parameters and the simulation method were validated. Within this stage, comparative analyses were performed for the path-dependent attenuation, for the source corner frequency and for the definition of the stratification of the local site conditions. A suitable formula was chosen for the attenuation, the sensitivity of the simulations at the source corner frequency was discussed, a profile for defining the local site conditions in the INCERC site was established, and it was shown that the use a geological profile of shallow depth does not generate the changes specific to the local site conditions and that the specific amplifications for the long corner periods observed in INCERC/Bucharest are produced by the entire sedimentary package that extends to the Cretaceous-specific geology (approximately 1 km). Based on these last observations the proposed method and parameters were tested, resulting in simulated accelerograms that incorporate very well all the features of real accelerograms.

Finally, eight earthquake scenarios were defined and based on them, accelerograms were simulated in the INCERC site (four scenarios specific to hazard analyses with maximum possible moment magnitude over the corresponding depth range and four scenarios specific to the design requirements according to the limit states and the importance classes of the buildings defined in P100-1/2013). It was observed that regarding the spectral composition the hazard level proposed by the seismic design code P100-1/2013 is lower for periods greater than 1 s compared to certain simulated accelerograms, with significantly higher spectral amplitudes for the periods up to at 2.75-3.0 s. For five out of the eight scenarios, the average corner period of the simulations exceeds the value proposed by the design code, the maximum value of the corner period of the simulations being 2.57 s. Regarding the peak accelerations, the simulated accelerograms record a decrease of the amplitudes of up to 200 cm/s² compared to the peak accelerations recorded at the bedrock level, the nonlinear behaviour of the local site conditions producing energy dissipation and spectral content modification towards a richer content of amplitudes corresponding to larger periods.

The 40 accelerograms simulated based on the design hypotheses (SLS for all buildings, ULS for buildings of importance-exposure category III, ULS for buildings of importance-exposure category II and ULS for buildings of importance-exposure category I) are annexed to the present paper in electronic format to provide the design engineers with an alternative method of defining the seismic action.

Simulated accelerograms can become an important resource in hazard analyses because they are generated taking into account the real (simplified) characteristics of the phenomena that generate and influence the seismic waves. Unlike the recorded and scaled accelerograms and compared to the artificial accelerograms, the simulated accelerograms better incorporate the influence of local site conditions. Simulated accelerograms can be performed for locations where there are no records of seismic motions, for historical earthquakes and for plausible hypothetical scenarios, and together with the recorded accelerograms can be a more complete database for hazard analysis.

The disadvantage of the simulated accelerograms (but at the same time the reason why they are more realistic) is given by the complexity and the multitude of parameters that define the

seismic motion, a thorough research being needed. The superficial research of the phenomena and parameters that generate and modify the seismic waves can lead to unrealistic results.

### Future research directions:

In the future, more complex investigations of the local site conditions are needed to determine the characteristics of the soil layers for deep geological profiles. Following these researches, simulations can be carried out for other sites. The parameters of the white noise shaping window could be determined for narrower databases defined according to local site conditions, topography, attenuation and directivity. It is of interest to study the phenomena that produce the observed changes in the accelerograms classified as exceptions in the energy release analysis. For the source corner frequency one should try to determine more accurate formulas, with narrower confidence intervals because the simulations are extremely sensitive to changes in this parameter. A number of parameters such as the path attenuation should be restudied because in their literature its definition is very varied. As a future direction of more complex research, it would be ideal to pursue a more thorough investigation of the phenomena that produce and modify seismic waves so that 3D simulations can be performed so that at least the topography is to be considered (given that under certain conditions, the seismic waves are greatly influenced by the topography).

#### 7. Bibliography

Aki, K., 1966. Generation and Propagation of G Waves from the Niigata Earthquake of June 16, 1964. Part 2. Estimation of Earthquake Moment, Released Energy, and Stress-strain Drop from the G-Wave Spectrum. *Bull. Earthq. Res. Inst. 44, 73–88.* 

Anderson, J. & Hough, S., 1984. A model for the shape of the Fourier amplitude spectrum of acceleration at high frequencies. *Bull Seism. Soc. Am. 74, 1969-1993*.

Atkinson, G. & Boore, D. M., 1995. New ground motion relations for eastern North America. Bull Seism. Soc. Am. 85, 17-30.

Benetatos, C. & Kiratzi, A., 2004. Stochastic strong ground motion simulation of intermediate depth earthquakes: The cases of the 30 May 1990 Vrancea (Romania) and of the 22 January 2002 Karpathos island (Greece) earthquakes, s.l.: Soil Dynamics and Earthquake Engineering 24(1):1-9.

Beresnev, I. & Atkinson, G., 1998. FINSIM — A FORTRAN Program for Simulating Stochastic Acceleration Time Histories from Finite Faults. *Seismol. Res. Lett.*, 69:27–32.

Besutiu, L., 2006. Alternative geodynamic model for Vrancea intermediate-depth seismicity: the unstable triple junction. In: Geodynamic studies in Romania - Vrancea zone. Monograph compiled in the frame of the Project CERGOP-2/Environt. *Reports on Geodesy, no.6* (81), 17-42, Warszawa.

Besutiu, L., Radulian, M., Zlagnean, L. & Atanasiu, L., 2009. Some peculiarities of the seismicity within the bending zone of the East Carpathians. Integrated research on the intermediate depth earthquake genesis within Vrancea zone. s.l.:Vergiliu Publishing Housem pp.36-111.ISBN978-973-7600-59-2.

Boore, D. M., 1983. Stochastic simulation of high-frequency ground motions based on seismological models of the radiated spectra. *Bull. Seismol. Soc. Am. 73*, 1865–18943.

Boore, D. M., 2003. Simulation of ground motion using the stochastic method. Pure Appl Geophys 160:635-676.

Boore, D. M., 2005. SMSIM-Fortran Programs for Simulating Ground Motions form Earthquakes. Version 7.04. U.S. Geol. Surv. Open-Field Report, p. 55.

Boore, D. M. & Joyner, W. B., 1997. Site amplifications for Generic Rock Sites. Bull. Seismol. Soc. Am. 87, pp. 327-341.

Boore, D. & Thompson, E., 2014. Path durations for use in the stochastic-method simulation of ground motions. *Bull. Seismol. Soc. Am.* 104, 2541--2552.

Brune, J. N., 1970. Tectonic stress and the spectra of seismic shear waves from earthquakes. J. Geophys. Res. 75, p. 997–5009.

Brune, J. N., 1971. Correction. J. Geophys. Res. 76, p. 5002.

Constantinescu, L. & Enescu, E., 1985. Vrancea earthquakes from scientific and technologic point of view. s.l.: Editura Academiei.

Cotovanu, A., 2018. Stochastic Simulation of Ground Motions Generated by Vrancea Intermediate-Depth Seismic Source. *Journal of Military Technology, vol.1, no.2, Dec. 2018, 10.32754/JMT.2018.2.05.* 

Coţovanu, A. & Vacareanu, R., 2019. Local site conditions modeling in stochastic simulation of ground motions generated by Vrancea (Romania) intermediate-depth seismic source. *Journal of Seismology, DOI: 10.1007/s10950-019-09892-5.* 

Coţovanu, A. & Vacareanu, R., 2020. Modeling energy release parameters in stochastic simulation of ground motions generated by Vrancea intermediate-depth seismic source. *Bulletin of Earthquake Engineering*.

Ganas, A., Grecu, B., Batsi, E. & Radulian, M., 2010. Vrancea slab earthquake triggerd by static stress transfer. *Nat. Hazards Earth Syst. Sci.*, 10, 2565–2577.

Gusev, A., Radulian, M., Rizescu, M. & Panza, G. F., 2002. Source scaling of intermediate-depth Vrancea earthquakes. *Geophysical Journal International, Volume 151, Issue 3*.

Haddon, R., 1996. Earthquake source spectra in Eastern North America. Bull. Seismol. Soc. Am. 86,1300-1313.

Hanks, T., 1979. Values and  $ω^{(-\gamma)}$  Seismic Source Models: Implications for Tectonic Stress Variations along Active Crustal Fault Zones and the Estimation of High-frequency Strong Ground Motion. *J. Geophys. Res.* 84, 2235–2242.

Hanks, T. C. & McGuire, R. K., 1981. The character of high-frequency strong ground motion. *Bull. Seismol. Soc. Am. 71, 2071–2095*. Hartzell, S. H., 1978. Earthquake aftershocks as Greens functions. *Geophys. Res. Lett. 5*.

Hashash, Y. şi alţii, 2016. DEEPSOIL 6.1, User Manual. *Urbana, IL, Board of Trustees of University of Illinois at Urbana-Champaign*. Hurukawa, N., Popa, M. & Radulian, M., 2008. Relocation of large intermediate-depth earthquakes in the Vrancea region, Romania, since 1934 and a seismic gap. *Earth Planets Space*, 60, 565–572.

Irikura, K., 1983. Semi-Empirical Estimation of Strong Ground Motions during Large Earthquakes. Bull. Dis. Prev. Res. Inst., Kyoto Univ., 33, Part 2, No. 298.

Irikura, K., 1986. Prediction of Strong Acceleration Motions Using Empirical Green's Function. Tokyo, s.n.

Irikura, K., 1999. *Techniques for the Simulation of Strong Ground Motion and Deterministic Seismic Hazard Analysis*. Kefallinia, Proceedings of the Advanced Study Course Seismotectonics and Microzonation Techniques in Earthquake Engineering: Integrated Training in Earthquake Risk Reduction Practices.

Irikura, K. & Miyake, H., 2006. Lecture note on Strong Motion Seismology. Trieste, Italy, Proc. of the 8th Workshop on Three-Dimensional Modeling of Seismic Waves Generation, Propagation and Their Inversion.

Ismail-Zadeh, A. și alții, 2012. Geodynamics and intermediate-depth seismicity in Vrancea (the south-eastern Carpathians): current state-of-the art. *Tectonophysics 530, 50-79*.

Kanamori, H., 1979. A semi-empirical approach to prediction of long-period ground motions from great earthquakes. *Bull. Seism. Soc. Am.*, 69, 1645-1670.

Karimzadeh, S., 2019. Seismological and Engineering Demand Misfits for Evaluating Simulated Ground Motion Records. *Applied Sciences* 9(21):4497.

Kotke, A. R. & Rathje, E. M., 2009. *Technical manual for Strata. PEER Report 2008/10*, Berkeley: Pacific Earthquake Engineering Research Center, College of Engineering, University of California.

Lungu, D. și alții, 1998. Surface geology and dynamic properties of soil layers in Bucharest, in Vrancea Earthquakes. *Tectonics, Hazard and Risk Mitigation, Kluwer Academic publisher, Wenzel F., Lungu D.-Editors.* 

Manea, V. C. și alții, 2011. *Studiu privind analiza modelelor geodinamice existente*, Programul Operațional Sectorial Creșterea Competitivității Economice: Proiect: Infrastructură cibernetică pentru studii geodinamice relaționate cu zona seismogenă Vrancea: ID-593, cod SMIS-CSNR 12499; Etapa 1: Construirea si testarea sistemului hardware (HPCC, HPVC si GeoWall).

Martin, M., Wenzel, F. & group, a. t. C. w., 2006. High-Resolution Teleseismic Body Wave Tomography Beneath SE-Romania (II): Imaging of a Slab Detachment Scenario. *Geophys. J. Int.*, 164:579–595.

McGuire, R. & Hanks, T., 1980. RMS Accelerations and Spectral Amplitudes of Strong Ground Motion during the San Fernando, California, Earthquake. *Bull. Seismol. Soc. Am. 70, 1907-1919*.

MDRAP, 2014. P100-1/2013 Cod de proiectare seismică – Partea I – Prevederi de proiectare pentru clădiri. București, România.: Ministerul Dezvoltării Regionale și Administrației Publice.

Miyake, H., Iwata, T. & Irikura, K., 2003. Source Characterization for Broadband Ground-Motion Simulation: Kinematic Heterogeneous Source Model and Strong Motion Generation Area. *Bulletin of the Seismological Society of America* (2003) 93 (6): 2531-2545.

Motazedian, D. & Atkinson, G. M., 2005. Stochastic Finite-Fault Modeling Based on a Dynamic Corner Frequency. *Bulletin of the Seismological Society of America, Vol. 95, No. 3*, June, p. 995–1010.

Neagu, C., 2015. Influența condițiilor locale de amplasament și a comportării neliniare a terenului asupra acțiunii seismic de proiectare. *Teză de doctorat, UTCB*.

Oncescu, M. C. & Bonjer, K.-P., 1997. A note on the depth recurrence and strain release of large Vrancea earthquakes. *Tectonophysics*, 272, 291-302.

Oncescu, M. C., Bonjer, K.-P. & Rizescu, M., 1999. Weak and strong ground motion of intermediate depth earthquakes from the Vrancea region. În: F. Wenzel, L. D. & N. O., ed. *Vrancea earthquakes: tectonics, hazard and risk mitigation.* Dordrecht, Netherlands: Kluwer Academic Publishers, pp. 27-42.

Oth, A., Bindi, D., Parolai, S. & Wenzel, F., 2008. S-Wave Attenuation Characteristics beneath the Vrancea Region in Romania: New Insights from the Inversion of Ground-Motion Spectra. *Bulletin of the Seismological Society of America*.

Oth, A., Parolai, S., Bindi, D. & Wenzel, F., 2009. Source spectra and site response from S waves of intermediate-depth Vrancea, Romania, earthquakes. *Bulletin of the Seismological Society of America* 99:235-254.

Oth, A., Wenzel, F. & Radulian, M., 2007. Source parameters of intermediate-depth Vrancea (Romania) earthquakes from empirical Green's functions modeling. *Tectonophysics* 438 (2007) 33–56.

Pavel, F., 2015. Investigation on the stochastic simulation of strong ground motions for Bucharest area. *Soil Dynamics and Earthquake Engineering* 69 (2015) 227–232.

Pavel, F., 2017. Investigation on the Variability of Simulated and Observed Ground Motions for Bucharest Area. *Journal Of Earthquake Engineering, DOI 10.1080/13632469.2017.1297266*.

Pavel, F., Popa, V. & Vacareanu, R., 2018. Evaluation of Soil Conditions in Bucharest. În: *Impact of Long-Period Ground Motions on Structural Design: A Case Study for Bucharest, Romania, DOI:10.1007/978-3-319-73402-6\_2.* s.l.:s.n.

Pavel, F. & Vacareanu, F., 2017. Ground motion simulations for seismic stations in southern and eastern Romania and seismic hazard assessment. *J Seismol, DOI 10.1007/s10950-017-9649-1*.

Pavel, F. & Vacareanu, R., 2015. Assessment of the ground motion levels for the Vrancea (Romania) November 1940 earthquake. *Nat Hazards, DOI 10.1007/s11069-015-1767-x*.

Pavel, F. & Vacareanu, R., 2015. Kappa and regional attenuation for Vrancea (Romania) earthquakes. *J Seismol. doi:10.1007/s10950-015-9490-3*.

Pavel, F. & Vacareanu, R., 2018. Investigation on regional attenuation of Vrancea (Romania) intermediate-depth earthquakes. *Earthq Eng & Eng Vib* (2018) 17: 501-509.

Pavel, F. și alții, 2017. Impact of spatial correlation of ground motions on seismic damage for residential buildings in Bucharest, Romania. Nat Hazards, Volumul 87, p. 1167–1187

Pavel, F. şi alţii, 2016. An Updated Probabilistic Seismic Hazard Assessment for Romania and Comparison with the Approach and Outcomes of the SHARE Project. *Pure and Applied Geophysics*, 173(6): 1881-1905.

Pitarka, A., 1999. 3D elastic finite-difference modeling of seismic wave propagation using staggered grid with non-uniform spacing. *Bull. Seism. Soc. Am.* 89, 54–68.

Poiata, E. & Miyake, H., 2017. Broadband Ground Motion Simulation of the 2004 and 1977 Vrancea, Romania, Earthquakes Using Empirical Green's Function Method. *Pure Appl. Geophys.*, Issue DOI 10.1007/s00024-017-1605-z.

Popescu, E., Radulian, M. P. M., Placinta, A. & Grecu, B., 2007. Source of Vrancea (Romania) intermediate-depth earthquakes: parameter variability test using a small-aperture array. *Rev. Roum. GEOPHYSIQUE*, *51*, *p. 15-34*, 2007, *Bucuresti*.

Radulian, M. și alții, 2019. Revised catalogue of earthquake mechanisms for the events occurred in Romania until the end of twentieth century: REFMC. *Acta Geodaetica et Geophysica 54(1):3-18*.

Radulian, M. și alții, 2000. Characterization of seismogenic zones of Romania.

Saragoni, G. R. & Hart, G. C., 1974. Simulation of artificial earthquakes. *Earthquake engineering and Structural dynamics*, pp. 249-267. Seed, H. & Idriss, I., 1970. Soil Moduli and Damping Factors for Dynamic Response Analyses. *Report EERC 70-10, Earthquake Engineering Research Center, University of California, Berkeley.* 

Sokolov, V. și alții, 2008. Ground-motion prediction equations for the intermediate depth Vrancea (Romania) earthquakes. *Bull Earthquake Eng* (2008) 6:367–388.

SR-EN1998-1:2004, 2004. Eurocod 8: Proiectarea structurilor pentru rezistenta la cutremur. Partea 1: Reguli, s.l.: s.n.

Vucetic, M. & Dobry, R., 1991. Effect of Soil Plasticity on Cyclic Response. Journal of Geotechnical Engineering, 117, 89-107.